J|A|C|S
ARTICLES
Published on Web 11/21/2002

Mechanism of the Hydrogenation of Ketones Catalyzed by *trans*-Dihydrido(diamine)ruthenium(II) Complexes†

Kamaluddin Abdur-Rashid,‡ Sean E. Clapham,‡ Alen Hadzovic,‡ Jeremy N. Harvey,§ Alan J. Lough,‡ and Robert H. Morris*,‡

Contribution from Davenport Laboratories, Department of Chemistry, University of Toronto, 80 St George St., Toronto, Ontario M5S 3H6, Canada, and School of Chemistry, University of Bristol, Cantock's Close, Bristol BS8 1TS, UK

Received August 10, 2001

Abstract: The complexes *trans*-RuH(Cl)(tmen)(*R*-binap) (**1**) and (OC-6−43)-RuH(Cl)(tmen)(PPh_3)$_2$ (**2**) are prepared by the reaction of the diamine $NH_2CMe_2CMe_2NH_2$ (tmen) with RuH(Cl)(PPh_3)(*R*-binap) and RuH(Cl)(PPh_3)$_3$, respectively. Reaction of $KHB^{sec}Bu_3$ with **1** yields *trans*-Ru(H)$_2$(*R*-binap)(tmen) (**5**) while reaction of $KHB^{sec}Bu_3$ or KO^tBu with **2** under Ar yields the new hydridoamido complex RuH(PPh_3)$_2$($NH_2CMe_2CMe_2$-NH) (**4**). Complex **4** has a distorted trigonal bipyramidal geometry with the amido nitrogen in the equatorial plane. Loss of H_2 from **5** results in the related complex RuH(*R*-binap)($NH_2CMe_2CMe_2NH$) (**3**). Reaction of H_2 with **4** yields the *trans*-dihydride (OC-6−22)-Ru(H)$_2$(PPh_3)$_2$(tmen) (**6**). Calculations support the assignment of the structures. The hydrogenation of acetophenone is catalyzed by **5** or **4** in benzene or 2-propanol without the need for added base. For **5** in benzene at 293 K over the ranges of concentrations [**5**] = 10^{-4} to 10^{-3} M, [ketone] = 0.1 to 0.5 M, and of pressures of H_2 = 8 to 23 atm, the rate law is rate = k[**5**][H_2] with k = 3.3 M^{-1} s^1, $\Delta H^{\ddagger}$ = 8.5 ± 0.5 kcal mol^{-1}, $\Delta S^{\ddagger}$ = −28 ± 2 cal mol^{-1} K^{-1}. For **4** in benzene at 293 K over the ranges of concentrations [**4**] = 10^{-4} to 10^{-3} M, [ketone] 0.1 to 0.7 M, and of pressures of H_2 = 1 to 6 atm, the preliminary rate law is rate = k[**4**][H_2] with $k = 1.1 \times 10^2$ M^{-1} s^{-1}, $\Delta H^{\ddagger}$ = 7.6 ± 0.3 kcal mol^{-1}, $\Delta S^{\ddagger}$ = −23 ± 1 cal mol^{-1} K^{-1}. Both theory and experiment suggest that the intramolecular heterolytic splitting of dihydrogen across the polar Ru═N bond of the amido complexes **3** and **4** is the turn-over limiting step. A transition state structure and reaction energy profile is calculated. The transfer of $H^{\delta+}/H^{\delta-}$ to the ketone from the RuH and NH groups of **5** in a Noyori metal−ligand bifunctional mechanism is a fast process and it sets the chirality as (*R*)-1-phenylethanol (62−68% ee) in the hydrogenation of acetophenone. The rate of hydrogenation of acetophenone catalyzed by **5** is slower and the ee of the product is low (14% *S*) when 2-propanol is used as the solvent, but both the rate and ee (up to 55% *R*) increase when excess KO^tBu is added. The formation of ruthenium alkoxide complexes in 2-propanol might explain these observations. Alkoxide complexes {RuP_2}H(OR)(tmen), {RuP_2} = Ru(*R*-binap) or Ru(PPh_3)$_2$, R= ^{i}Pr, CHPhMe, ^{t}Bu, are observed by reacting the alcohols ^{i}PrOH, phenylethanol, and ^{t}BuOH with the dihydrides **5** and **6**, respectively, under Ar. In the absence of H_2, the amido complexes **3** and **4** react with acetophenone to give the ketone adducts {RuP_2}H(O═CPhMe)($NH_2CMe_2CMe_2NH$) in equilibrium with the enolate complexes *trans*-{RuP_2}(H)(OCPh═CH_2)(tmen) and eventually the decomposition products {RuP_2}H(η^5-CH_2-CPhCHCPhO), with the binap complex characterized crystallographically. In general, proton transfer from the weakly acidic molecules dihydrogen, alcohol, or acetophenone to the amido nitrogen of complexes **3** and **4** is favored in two ways when the molecule coordinates to ruthenium: (1) an increase in acidity of the molecule by the Lewis acidic metal and (2) an increase in the basicity of the amido nitrogen caused by its pyramidalization. The formato complexes *trans*-{RuP_2}H(OCHO)(tmen) were prepared by reacting the respective complex **4** or **5** with formic acid. The crystal structure of RuH(OCHO)(PPh_3)$_2$(tmen) displays similar features to the calculated transition state for $H^{\delta+}/H^{\delta-}$ transfer to the ketone in the catalytic cycle.

Introduction

Noyori and co-workers have developed very active and selective ruthenium catalysts for the hydrogenation or asymmetric hydrogenation of ketones.[1,2] The ruthenium catalysts are usually generated in a 2-propanol solution by mixing a ruthenium dichloride precursor complex with an excess of a strong base such as potassium *tert*-butoxide under dihydrogen in the presence of the ketone substrate. The ruthenium complexes *trans*-$RuCl_2$(PPh_3)$_2$(diamine) or *trans*-$RuCl_2$(diphosphine)-(diamine) contain monodentate or chiral bidentate phosphine

* Corresponding author e-mail: rmorris@chem.utoronto.ca.
† Part of this work was presented at the Canadian Society for Chemistry Conference, Montreal, May 2001.
‡ University of Toronto.
§ University of Bristol.

(1) Noyori, R.; Ohkuma, T. *Angew. Chem., Int. Ed.* **2001**, *40*, 40−73.
(2) Noyori, R.; Yamakawa, M.; Hashiguchi, S. *J. Org. Chem.* **2001**, *66*, 7931−7944.

10.1021/ja016817p CCC: $22.00

Chart 1

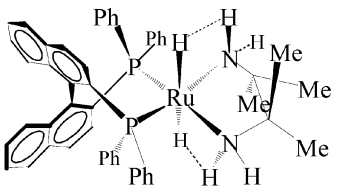

(a) Ru(*R*-binap)(H)$_2$(tmen) (5)

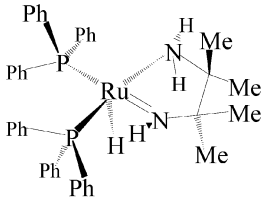

(b) Ru(PPh$_3$)$_2$H(NH$_2$CMe$_2$CMe$_2$NH) (4)

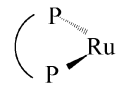

(c) {RuP$_2$}

ligands, especially the binap ligand, and also an achiral or chiral diamine ligand such as dpen = 1,2-diamino-1,2-diphenylethane and cydn = 1,2-diaminocyclohexane. Noyori and co-workers have shown that the amino group is crucial to the activity of the hydrogenation catalyst. They note that at least 2 equiv of an alkoxide base are needed to neutralize HCl that is formed in the catalyst activation. They speculate that a hydride complex with a *fac*-hydrido(diamine)Ru substructure of the form RuH(diamine)(PR$_3$)$_2$(X), where X is hydride, alkoxide, or some other anion, is responsible for an unconventional transfer of dihydrogen from the hydride on ruthenium and a hydrogen on a diamine amino group to the ketone to give the alcohol product.[1] Noyori has coined the phrase metal−ligand bifunctional catalysis to describe this dihydrogen transfer catalysis.[2] It was first observed by their research group for a different solvent-transfer hydrogenation catalyst, RuH(cymene)(*S*,*S*-H$_2$NCHPhCHPhNSO$_2$-tol),[3] and later studied by others.[4−7] Dihydrogen transfer from RuH(diamine)(PR$_3$)$_2$(X) to the ketone is proposed to result in the formation of an amido complex Ru(aminoamido)(PR$_3$)$_2$(X) that, in turn, is thought to react with dihydrogen to re-form RuH(diamine)(PR$_3$)$_2$(X). They also suggest that the activation of dihydrogen is the turn-over limiting step in this cycle in view of the marked dependency of the rate on hydrogen pressure.[1]

Recently Hartmann and Chen showed that a basic 2-propanol solution created by the addition of excess DBU is not sufficient to activate the ruthenium dichloride precursors *trans*-RuCl$_2$(*R*-binap)(*R*,*R*-dpen) for the catalytic hydrogenation of acetophenone; a source of potassium ion is also needed.[8] They suggest that the role of the potassium counterion of the alkoxide base in 2-propanol is to coordinate to the amido nitrogen of an intermediate and act as a Lewis acid to assist in the activation of dihydrogen.

The research of some of us showed that the X ligand in these catalytic intermediates RuH(diamine)(PR$_3$)$_2$(X) and Ru(aminoamido)(PR$_3$)$_2$(X) is likely to be hydride.[5,9] We provided evidence for a mechanism for the hydrogenation of ketones that involves the transfer of H$^{\delta-}$/H$^{\delta+}$ equivalents from the crystallographically characterized *cis*-dihydride catalyst (OC-6−13)-Ru(H)$_2$(PPh$_3$)$_2$(cydn), cydn = (*R*,*R*)-1,2-diaminocyclohexane,[5,10] and *trans*-dihydride catalyst Ru(H)$_2$(*R*-binap)(tmen), tmen = NH$_2$CMe$_2$CMe$_2$NH$_2$ (**5**),[9] to ketones and the heterolytic splitting of dihydrogen at the amido intermediates Ru(H)(PPh$_3$)$_2$(cydnamido)[5] and Ru(H)(*R*-binap)(NH$_2$CMe$_2$CMe$_2$NH) (**3**)[9] (see Table 1 and Chart 1 for the numbering scheme for the complexes of the current study). These were shown to be very active catalysts for ketone and imine hydrogenation in neat substrate or benzene solution without the requirement of added base. As the reaction progresses, the solvent is converted to alcohol or amine but the catalysts continue to function. Related dihydrides *trans*-Ru(H)$_2$(*R*,*R*-dpen)(*R*-binap), *trans*-Ru(H)$_2$(*R*-daipen)(*R*-binap), and *trans*- Ru(H)$_2$(*R*,*R*-cydn)(*R*-binap) have been observed by NMR.[9] These are of direct relevance to the species generated in situ from the Noyori dichloride catalyst precursors *trans*-RuCl$_2$(diamine)(*R*-binap), diamine = *R*,*R*-dpen, *R*-daipen, and *R*-cydn, respectively, but are very reactive and tend to decompose by various C−H bond activation mechanisms.[9,11] The use of the tmen ligand that contains no hydrogens α to the amino groups allowed us to isolate **3**, the first aminoamidohydride complex. However, crystals of this important amido complex were not available for an X-ray diffraction study. The NH$_2$CMe$_2$CMe$_2$NH ligand has been observed previously in the aminoamido complex [Ru(bipy)(NHCMe$_2$CMe$_2$NH$_2$)$_2$](ZnBr$_4$).[12]

Late transition metal amido complexes have proven to be very reactive[13−16] and have been identified as important intermediates in both stoichiometric and catalytic reactions.[15] They were first identified in mechanisms involving base-

Table 1. Numbering of the Complexes of This Study

	{RuP$_2$} =	
complex	Ru(*R*-binap)	Ru(PPh$_3$)$_2$
trans-{RuP$_2$}(H)(Cl)(tmen)	**1**	**2**
{RuP$_2$}(H)(NH$_2$CMe$_2$CMe$_2$NH)	**3**	**4**
trans-{RuP$_2$}(H)$_2$(tmen)	**5**	**6**
{RuP$_2$}(H)(O=CMePh)(NH$_2$CMe$_2$-CMe$_2$NH)	**7**	**8**
trans-{RuP$_2$}(H)(OCPh=CH$_2$)(tmen)	**9**	**10**
{RuP$_2$}H(η^5-CH$_2$CPhCHCPhO)	**11**	**12**
{RuP$_2$}(H)(HOR)(NH$_2$CMe$_2$-CMe$_2$NH)	**13a**, **13b**, **13c**[a]	**14a**, **14b**, **14c**[a]
trans-{RuP$_2$}(H)(OR)(tmen)	**15a**, **15b**, **15c**[a]	**16a**, **16b**, **16c**[a]
trans-{RuP$_2$}H(OCHO)(tmen)	**17**	**18**

[a] R= CHMePh (**a**), ^{t}Bu (**b**), ^{i}Pr (**c**).

(3) Haack, K. J.; Hashiguchi, S.; Fujii, A.; Ikariya, T.; Noyori, R. *Angew. Chem., Int. Ed. Engl.* **1997**, *36*, 285−288.
(4) Casey, C. P.; Singer, S. W.; Powell, D. R.; Hayashi, R. K.; Kavana, M. *J. Am. Chem. Soc.* **2001**, *123*, 1090−1100.
(5) Abdur-Rashid, K.; Lough, A. J.; Morris, R. H. *Organometallics* **2000**, *19*, 2655−2657.
(6) Alonso, D. A.; Brandt, P.; Nordin, S. J. M.; Andersson, P. G. *J. Am. Chem. Soc.* **1999**, *121*, 9580−9588.
(7) Bernard, M.; Delbecq, F.; Sautet, P.; Fache, F.; Lemaire, M. *Organometallics* **2000**, *19*, 5715−5722.
(8) Hartmann, R.; Chen, P. *Angew. Chem., Int. Ed.* **2001**, *40*, 3581−3585.
(9) Abdur-Rashid, K.; Faatz, M.; Lough, A. J.; Morris, R. H. *J. Am. Chem. Soc.* **2001**, *123*, 7473−7474.
(10) Geoffroy, G. L. Inorganic and Organometallic Stereochemistry. In *Topics in Stereochemistry*, Vol. 12; Allinger, N. L., Eliel, E. L., Eds.; Wiley: New York, 1981.
(11) Abbel, R.; Abdur-Rashid, K.; Clapham, S.; Eberhardt, M.; Lough, A. J.; Morris, R. H., manuscript in preparation.
(12) Chiu, W.-H.; Peng, S.-M.; Che, C.-M. *Inorg. Chem.* **1996**, *35*, 3369−3374.
(13) Bryndza, H. E.; Tam, W. *Chem. Rev.* **1988**, *88*, 1163−1188.
(14) Fryzuk, M. D.; Montgomery, C. D. *Coord. Chem. Rev.* **1989**, *95*, 1−40.
(15) Fulton, J. R.; Holland, A. W.; Fox, D. J.; Bergman, R. G. *Acc. Chem. Res.* **2002**, *35*, 44−56.
(16) Fulton, J. R.; Bouwkamp, M. W.; Bergman, R. G. *J. Am. Chem. Soc.* **2000**, *122*, 8799−8800.

Scheme 1. Proposed Mechanism for the Catalytic Hydrogenation of Ketones Catalyzed by the *trans*-Dihydride Complexes **5** and **6** or the Hydridoamido Complexes **3** and **4**

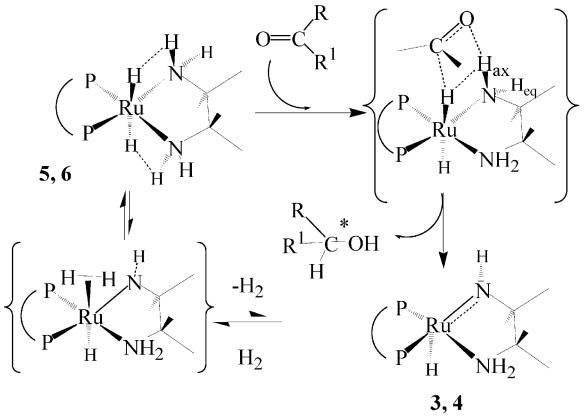

catalyzed substitution reactions at substitution-inert amine complexes; for example, $[CoCl(NHCH_2CH_2NH_2)(en)]^+$ is an intermediate in the base-catalyzed aquation of $[CoCl_2(en)_2]^+$.[17] More recently they have gained prominence as extremely strong bases in carbon−hydrogen bond activation reactions[16] and as intermediates in the catalytic hydroamination of arylhalides[18] and hydrogen-transfer hydrogenation[3,6,19−23] or direct hydrogenation of imines[5,24] and ketones as mentioned above.[1,5,9]

Here we report in more detail the mechanism of ketone hydrogenation catalyzed by the well-defined complexes **3** and **5** and the new complexes $RuH(PPh_3)_2(NH_2CMe_2CMe_2NH)$ (**4**) and *trans*-$Ru(H)_2(PPh_3)_2$(tmen) (**6**). Structures of catalysts **5** and **4** that contain the tmen diamine ligand and $NH_2CMe_2CMe_2NH$ aminoamido ligand, respectively, are shown in Chart 1. Since the chemistry of the two classes of complexes, one containing the Ru(*R*-binap) substructure and the other the $Ru(PPh_3)_2$ substructure, are very similar, we will denote them generically as $\{RuP_2\}$ as indicated in Chart 1, part (c).

The mechanism proposed for the dihydride catalyst **5** is shown in Scheme 1.[9] Our earlier work showed that the dihydride complex **5** reacts with a ketone to produce the alcohol and novel aminoamido complex Ru(*R*-binap)(H)($NH_2CMe_2CMe_2NH$) (**3**) in the unconventional second-coordination sphere transfer of dihydrogen as first proposed by Noyori and co-workers. It is postulated from the X-ray crystal structure determination of the dihydride **5** that only the axial NH that is aligned with the ruthenium hydride, possibly by a protonic−hydridic NH···HRu interaction,[25−27,28] is transferred to the ketone. The stereochemistry of this transition state is responsible for the observed enantioselectivity of the asymmetric hydrogenation of acetophenone to 1-phenylethanol as will also be discussed below.[9] We showed that dihydrogen adds across the Ru═N bond of the hydridoamido complex **3** to regenerate the dihydride in a reversible fashion. We postulated that an unobserved dihydrogen complex might act as an intermediate. The direct observation of such a reversible intramolecular heterolytic splitting of dihydrogen is rare,[29,30] and it is not only important in hydrogenation catalysis but also in biology.[31,32] The irreversible reaction of the related 16-electron, silyl-stabilized amido complex $Ru(Cl)\{N(SiMe_2CH_2PPh_2)_2\}(PPh_3)$ with dihydrogen gives an amino hydride complex,[33] possibly via a dihydrogen complex.[34] The current work describes the structure determination of the amido complex **4** and suggests that it is the heterolytic splitting of the dihydrogen at the amido complex that is the turn-over limiting step in catalysis. These conclusions are supported by calculation (in fact the identity of the turnover limiting step was successfully predicted in this way). Other reactions of the complexes **3**−**6** with the reactant ketone and product alcohol have been identified and may play a role in the catalysis under certain conditions as will be described below.

Results

***trans*-{RuP$_2$}(H)(Cl)(tmen).** The precursors to the catalysts are the hydridochloro complexes *trans*-RuH(Cl)(tmen)(*R*-binap) (**1**) and $RuH(Cl)(tmen)(PPh_3)_2$ (**2**). These were prepared in a fashion similar to related *trans*-RuH(Cl)(diphosphine)(diamine) and $RuH(Cl)(PPh_3)_2$(diamine) complexes[24] by reacting the suitable complex $\{RuP_2\}H(Cl)(PPh_3)$ with tmen. These were characterized by elemental analysis, NMR, IR, and X-ray crystallography. The complexes are yellow solids that are moderately stable in air but react with air when dissolved in THF or acetone. The complexes have the OC-6−43 configuration[10] with hydride *trans* to chloride (Scheme 2). A small amount of an insoluble, deeply colored complex is also produced with **2**; this complex is thought to have the OC-6−23 configuration with *cis*-$\{RuP_2\}$ and *cis*-RuH(Cl) substructures as will be described elsewhere.

The spectroscopic properties and crystal structure of **1** have been reported.[9] The five-member ring formed by the tmen ligand in **1** is in the δ configuration with axial and equatorial N−H groups. The chloride ligand forms an intramolecular hydrogen bond with an axial NH of the tmen ligand (Scheme 2) as is observed also in RuH(Cl)(*R*-dpen)(*R*-binap).[24]

Similarly, the complex $RuH(Cl)(PPh_3)_2$(tmen) (**2**) in solution and in the crystalline state has *cis* phosphine groups and hydride *trans* to chloride as in other complexes of this type (Figure 1).[5,24,35] Again there is an intramolecular Cl···HN hydrogen bond with a Cl···H distance of 2.6 Å. The ^{1}H (hydride) and ^{31}P NMR spectra show that **1** and **2** have a *fac*-$\{RuP_2\}(H)$ substructure. Rapid flipping of the Ru(tmen) ring results in only two NH and two CMe proton signals for **2** in contrast to the four NH and four CMe signals observed for rigid complex **1**.

(17) Basolo, F.; Pearson, R. G. *Mechanisms of Inorganic Reactions*; Wiley: New York, 1967.
(18) Alcazar-Roman, L. M.; Hartwig, J. F.; Rheingold, A. L.; Liable-Sands, L. M.; Guzei, I. A. *J. Am. Chem. Soc.* **2000**, *122*, 4618−4630.
(19) Yamakawa, M.; Ito, H.; Noyori, R. *J. Am. Chem. Soc.* **2000**, *122*, 1466−1478.
(20) Aitali, M.; Allaoud, S.; Karim, A.; Meliet, C.; Mortreux, A. *Tetrahedron: Asymmetry* **2000**, *11*, 1367−1374.
(21) Mashima, K.; Abe, T.; Tani, K. *Chem. Lett.* **1998**, 1199−1200.
(22) Thorpe, T.; Blacker, J.; Brown, S. M.; Bubert, C.; Crosby, J.; Fitzjohn, S.; Muxworthy, J. P.; Williams, J. M. J. *Tetrahedron Lett.* **2001**, *42*, 4041−4043.
(23) Mao, J.; Baker, D. C. *Org. Lett.* **1999**, *1*, 841−843.
(24) Abdur-Rashid, K.; Lough, A. J.; Morris, R. H. *Organometallics* **2001**, *20*, 1047−1049.
(25) Stevens, R. C.; Bau, R.; Milstein, D.; Blum, O.; Koetzle, T. F. *J. Chem. Soc., Dalton Trans.* **1990**, 1429−1432.
(26) Lough, A. J.; Park, S.; Ramachandran, R.; Morris, R. H. *J. Am. Chem. Soc.* **1994**, *116*, 8356−8357.
(27) Peris, E.; Lee, J. C.; Crabtree, R. H. *J. Chem. Soc., Chem. Commun.* **1994**, 2573.
(28) Also known as dihydrogen bonding. See articles in *Recent Advances in Hydride Chemistry*; Peruzini, M., Poli, R., Eds.; Elsevier: New York, 2001.
(29) Schlaf, M.; Lough, A. J.; Morris, R. H. *Organometallics* **1996**, *15*, 4423−4436.
(30) Schlaf, M.; Morris, R. H. *J. Chem. Soc., Chem. Commun.* **1995**, 625−626.
(31) Fan, H. J.; Hall, M. B. *J. Biol. Chem.* **2001**, *6*, 467−473.
(32) Fan, H. J.; Hall, M. B. *J. Am. Chem. Soc.* **2001**, *123*, 3828−3829.
(33) Fryzuk, M. D.; Montgomery, C. D.; Rettig, S. J. *Organometallics* **1991**, *10*, 467−473.
(34) Morris, R. H. *Inorg. Chem.* **1992**, *31*, 1471−1478.
(35) James, B. R.; Wang, D. K. W. *Inorg. Chim. Acta* **1976**, *19*, L17−L18.

Scheme 2. Preparation of the Hydridoamido Complexes **3** and **4** by a Dehydrochlorination Reaction (a) or Elimination of Dihydrogen (c) and the *trans*-Dihydride Complexes **5** and **6** by the Addition of Hydride (b) or Dihydrogen (c)

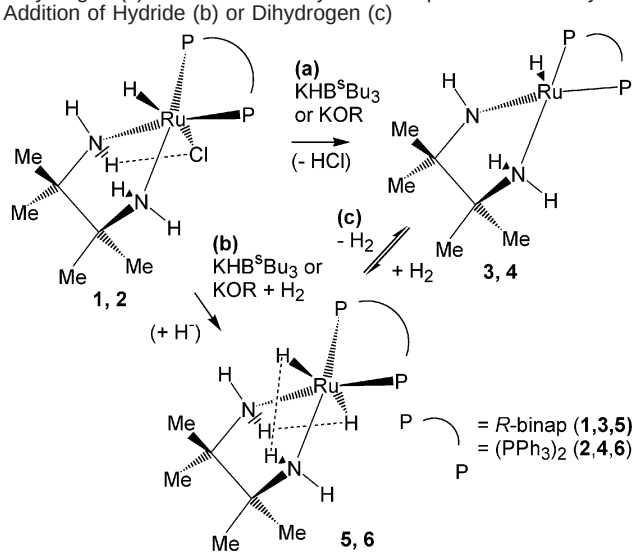

{**RuP$_2$**}**(H)(NH$_2$CMe$_2$CMe$_2$NH).** The dark red ruthenium hydridoamido complex, Ru(H)(*R*-binap)(NH$_2$CMe$_2$CMe$_2$NH) (**3**), was prepared in a dehydrochlorination reaction by reacting **1** with KO^{t}Bu or KO^{i}Pr in THF under Ar or in a dihydrogen elimination reaction by refluxing a THF solution of Ru(H)$_2$(*R*-binap)(tmen) (**5**) under Ar (Scheme 2). This complex was characterized by NMR as described elsewhere.[9] It has three inequivalent NH proton resonances at 1.22, 2.80, and 3.39 ppm and a broad triplet hydride resonance at −19.2. The CMe resonances in the ^{1}H NMR spectrum and the two inequivalent ^{31}P resonances are broadened by a fluxional exchange process of this five-coordinate complex. The IR spectrum shows two Ru−H vibrations at 2000 and 1953 cm^{-1} and two NH vibrations at 3332 and 3276 cm^{-1}. The higher NH wavenumber may be associated with the amido group; the complex RuH(NH$_2$)(dmpe)$_2$ has an NH stretch at 3504 cm^{-1}.[36]

The dehydrochlorination of **2** by reaction with a base such as KO^{t}Bu or K[BH(^{sec}Bu)$_3$] in THF under Ar leads to the orange, oxygen-sensitive hydridoamido complex RuH(PPh$_3$)$_2$(NH$_2$CMe$_2$CMe$_2$NH) (**4**) (Scheme 2). The dihydride RuH$_2$(PPh$_3$)$_2$(tmen) (see below) also readily loses H$_2$ in solution under Ar to produce **4**. The triplet hydride ^{1}H NMR pattern at −21.1 and singlet ^{31}P{^{1}H} pattern at 72.4 ppm indicate that the complex is fluxional in solution since the solid-state structure shows that there should be two inequivalent ^{31}P. There is a unique NH ^{1}H NMR resonance at 3.4 ppm for the amido NH while the two amino NH give a broadened resonance at 2.4 ppm. The amido N−H stretch appears at 3331 cm^{-1} for this complex while the Ru−H is at 1896 cm^{-1}. Solutions of complex **4** are sensitive to dinitrogen and decompose under 1 atm of N$_2$ to a dimeric dinitrogen complex that will be described elsewhere.[11]

In crystals, **4** exists as a distorted trigonal bipyramid (Figure 2) with the amido nitrogen equatorial and the amino nitrogen axial and approximately *trans* to a PPh$_3$ ligand (N(1)−Ru(1)−P(2) 165.0(1)°). The amido nitrogen−ruthenium distance is 1.967(1) Å (N(2)−Ru(1)), shorter than the amino nitrogen−ruthenium bond of 2.176(1) Å (N(1)−Ru(1)). The amido−ruthenium distance of **4** is longer than ones observed in Ru(cymene)(*S*,*S*-HNCHPhCHPhNSO$_2$tol) (1.897(6) Å)[3] and [Ru(bipy)(NH$_2$CMe$_2$CMe$_2$NH)$_2$]$^{2+}$ (1.856(6) Å) and between those of [Ru(tmen)(NH$_2$CMe$_2$CMe$_2$NH)$_2$]$^{2+}$ (1.835 Å, 2.093 Å).[12] The hydride ligand and other PPh$_3$ ligand are located in the equatorial plane with a small mutual angle with Ru (H(1RU)−Ru(1)−P(1) 79.2(8)°) and large angles to the amido nitrogen (H(1RU)−Ru−N(2) 128.0(8)°, P(1)−Ru−N(2) 151.4(1)°). The complex **3** also likely adopts a similar distorted trigonal bipyramidal geometry although the P−Ru−P angle will be reduced from 99.2° in **4** to a typical bite angle for the binap ligand of about 90°.

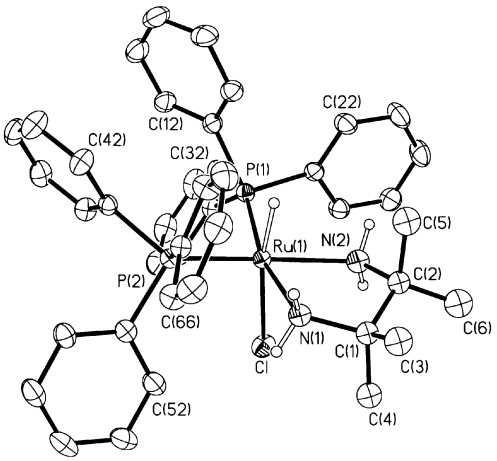

Figure 1. Molecular structure of RuH(Cl)(PPh$_3$)$_2$(tmen) (**2**).

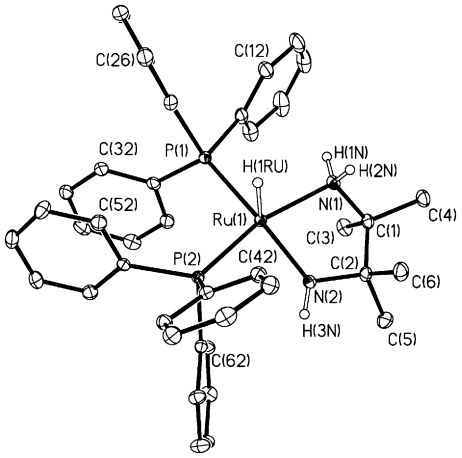

Figure 2. Crystal structure of Ru(PPh$_3$)$_2$H(NH$_2$CMe$_2$CMe$_2$NH) (**4**).

Calculations on Amido Model Complexes. The structures and energetics of the isomers of the model amido complex Ru(PH$_3$)$_2$H(NHCH$_2$CH$_2$NH$_2$) (**4′**) were examined by use of DFT (B3LYP) calculations. We have found only one low-lying isomer, with the others at least 30 kcal/mol higher in energy. This structure can be described either as a distorted square pyramid or as a distorted trigonal bipyramid (Figure 3). An optimized, complete structure of **4** was also calculated (Figure 3) and was found to be remarkably similar to the experimental one (Figure 2) and only slightly different from that of the model system with PH$_3$ and NHCH$_2$CH$_2$NH$_2$ ligands.

The relationship of the amido to the dihydride structure (Schemes 1, 2) is best discussed in octahedral terms, in which one has simply removed one of the hydrides and a neighboring pseudoaxial N−H proton from the *trans* hydride isomer of the

(36) Kaplan, A. W.; Ritter, J. C. M.; Bergman, R. G. *J. Am. Chem. Soc.* **1998**, *120*, 6828−6829.

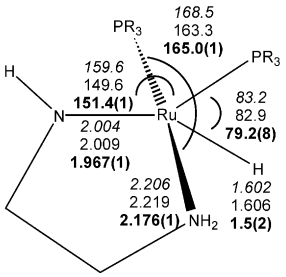

Figure 3. Selected computational and experimental bond lengths (Å) and angles (degrees) for Ru hydridoamido complexes. In italics: the model system **4′** (PH_3, $NHCH_2CH_2NH_2$) as computed. Plain text: the core of complex **4** as computed (Me and Ph groups not shown). Bold text: the core of the structure of complex **4** from the X-ray diffraction experiment.

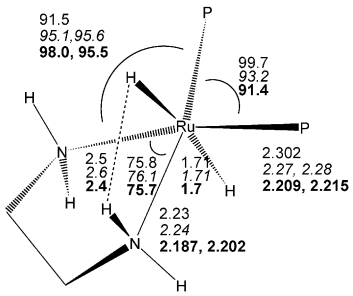

Figure 4. Selected computational and experimental bond lengths (Å) and angles (degrees) for the core of the Ru dihydride complexes. In plain text: **6** computed. Italic text: complex **5**, computed. Bold text: complex **5**, experimental.

Table 2. Computed Energetics (kcal mol^{-1}) of Isomeric Ruthenium Dihydride Complexes

$Ru(H)_2(L)_2$(diamine)	H_3P, en[a]	H_3P, en[b]	Ph_3P, en[c]	Ph_3P, tmen (**6**)[c]
trans $(H)_2$, *cis* $(L)_2$	0.0	0.0	0.0	0.0
cis $(H)_2$, *trans* $(L)_2$	−3.0	−4.4	−6.7	2.8
cis $(H)_2$, *cis* $(L)_2$	−6.1	−6.2	0.6	3.3

[a] B3LYP/BS A. [b] B3LYP/BS B//B3LYP/BS A + ZPE. [c] B3LYP/BS C.

dihydride. Thus there are minor structural changes on going from *trans*-$Ru(PH_3)_2(H)_2$(en) to the model amido compound.

The formal double bond between the amido nitrogen and ruthenium leads to a significantly shorter nitrogen−ruthenium distance than that for the amino nitrogen. The Y-shaped (deformed toward T-shaped) equatorial geometry of the distorted trigonal bipyramid is common for five-coordinate d^6 metal complexes containing one π-donor (X^-) and 4 σ-donor atoms (e.g., $Ir(OCH_2CF_3)(H)_2(PCy_3)_2$[37] and $[RuCl(dppe)_2]^+$ [38]) where X is equatorial at the base of the "Y" and uses an active lone pair in a p-type orbital to form a dative π-bond with the d_{xy} orbital.[39] The nitrogen in the amido ligand in **4** adopts a planar configuration so as to maximize this π-bonding.

***trans*-{RuP_2}$(H)_2$(tmen).** The complexes *trans*-{RuP_2}(H)(Cl)(tmen) (**1** or **2**) in THF or benzene react with a strong base and dihydrogen ($K[HB^{sec}Bu_3]/H_2$ or KO^iPr/H_2) to produce the yellow *trans*-dihydride complexes *trans*-$Ru(H)_2$(*R*-binap)(tmen) (**5**) or (OC-6−22)-$Ru(H)_2(PPh_3)_2$(tmen) (**6**) (Scheme 2). Complex **5** in solution under Ar slowly loses H_2 to give the amido complex **3**. Reaction of **3** in solution with H_2 rapidly produces **5** (Schemes 1, 2). The reaction of the amido complex **4** with H_2 in solution readily produces the *trans*-dihydride **6**, but this complex is much less stable than dihydride **5** with respect to the loss of H_2. Dihydride **6** under Ar loses H_2 readily in solution and in the solid state.

A single-crystal X-ray diffraction structure determination of $Ru(H)_2$(*R*-binap)(tmen) revealed an approximately C_2-symmetric, octahedral complex as described previously.[9] The tmen ligand forms a five-membered ring in the δ conformation with two sets of axial groups $N-H_{ax}$ and $C-Me_{ax}$ and two sets of equatorial groups $N-H_{eq}$ and $C-Me_{eq}$. The $RuH\cdots H_{ax}N$ distances of about 2.4 Å are at the outer limit of protonic−hydridic bonding.[25−28,40] Some metrical parameters for **5** are displayed in Figure 4.

The trans disposition of the hydride ligands in $Ru(H)_2$(*R*-binap)(tmen) and $Ru(H)_2(PPh_3)_2$(tmen) in solution is established by NMR. The temperature-independent triplet at −4.8 ppm in the ^1H NMR and singlet or triplet at 89.9 ppm in the $^{31}P\{^1H\}$ or ^{31}P NMR spectra, respectively, of $Ru(H)_2$(*R*-binap)(tmen) in solution are unambiguous for a trans structure. The triplet hydride resonance and singlet $^{31}P\{^1H\}$ resonance of $Ru(H)_2(PPh_3)_2$(tmen) could be consistent with *cis* hydrides and *trans* PPh_3 (OC-6−13) as found in $Ru(H)_2(PPh_3)_2$(cydn) ($\delta(Ru^1H)$ −18.2)[5] or *trans*-hydrides and *cis*-PPh_3 (OC-6−22). However, the hydride chemical shift of $Ru(H)_2(PPh_3)_2$(tmen) ($\delta(Ru^1H)$ −5.50) suggests the latter stereochemistry by analogy to complexes *trans*-RuH_2(diphosphine)(diamine) that have hydride chemical shifts in the region from −4.5 to −6.1 ppm.[9] The stereochemistry of $Ru(H)_2(PPh_3)_2$(tmen) with *trans*-hydrides was established by reacting $RuH(PPh_3)_2(NH_2CMe_2CMe_2NH)$ in C_6D_6 with D_2(g) to form the isotopomers $RuH(D)(PPh_3)_2$(tmen-d_x), $x = 0-4$ with D on ruthenium and nitrogen. The *trans*-$RuH(D)(PPh_3)_2$(tmen-d_x) isotopomers produce overlapping triplets for the hydrides in the ^1H NMR spectrum at −5.38 ppm. This large downfield shift of 0.12 ppm relative to undeuterated $Ru(H)_2(PPh_3)_2$(tmen) is caused by the large *trans* influence of deuterium. This proves that the hydrides are *trans* in the dihydride since a deuterium *cis* to a hydride would not have such a large influence on the chemical shift. The related isotopomers *trans*-$RuH_2(PPh_3)_2$(tmen-d_x) give overlapping triplets at −5.44 ppm, a downfield isotope shift of 0.06 ppm. The exchange of NH for ND during the reaction of $Ru(H)_2$(*R*-binap)(tmen) or $RuH(PPh_3)_2(NH_2CMe_2CMe_2NH)$ in C_6D_6 with D_2 is expected on the basis of the reversible interconversion of the complexes {RuP_2}$H(NH_2CMe_2CMe_2NH)$ and {RuP_2}H_2(tmen) under H_2/D_2 (Scheme 2).

Calculations on Dihydride Model Complexes. A calculation of the structures and energetics of the isomers of $Ru(PH_3)_2(H)_2$(en) (**6′**) and $Ru(PPh_3)_2(H)_2$(en) indicate that the isomer with *trans*-hydrides is highest in energy as described elsewhere.[41] The increased steric bulk of the diamine in $Ru(H)_2(PPh_3)_2$(tmen) (**6**) causes a destabilization of isomers with axial phosphines, leaving the complex with two axial hydrides as the most stable one, in agreement with our experimental observation (Table 2).

The core of the calculated structures of the dihydrides **5** and **6** is shown in Figure 4. Also included are dimensions from the

(37) Lunder, D. M.; Lobkovsky, E. B.; Streib, W. E.; Caulton, K. G. *J. Am. Chem. Soc.* **1991**, *113*, 1837−1838.
(38) Chin, B.; Lough, A. J.; Morris, R. H.; Schweitzer, C. T.; D'Agostino, C. *Inorg. Chem.* **1994**, *33*, 6278−6288.
(39) Riehl, J. F.; Jean, Y.; Eisenstein, O.; Pélissier, M. *Organometallics* **1992**, *11*, 729−737.
(40) Crabtree, R. H.; Siegbahn, P. E. M.; Eisenstein, O.; Rheingold, A. L. *Acc. Chem. Res.* **1996**, *29*, 348−354.
(41) Abdur-Rashid, K.; Harvey, J. N.; Lough, A. J.; Morris, R. H., manuscript in preparation.

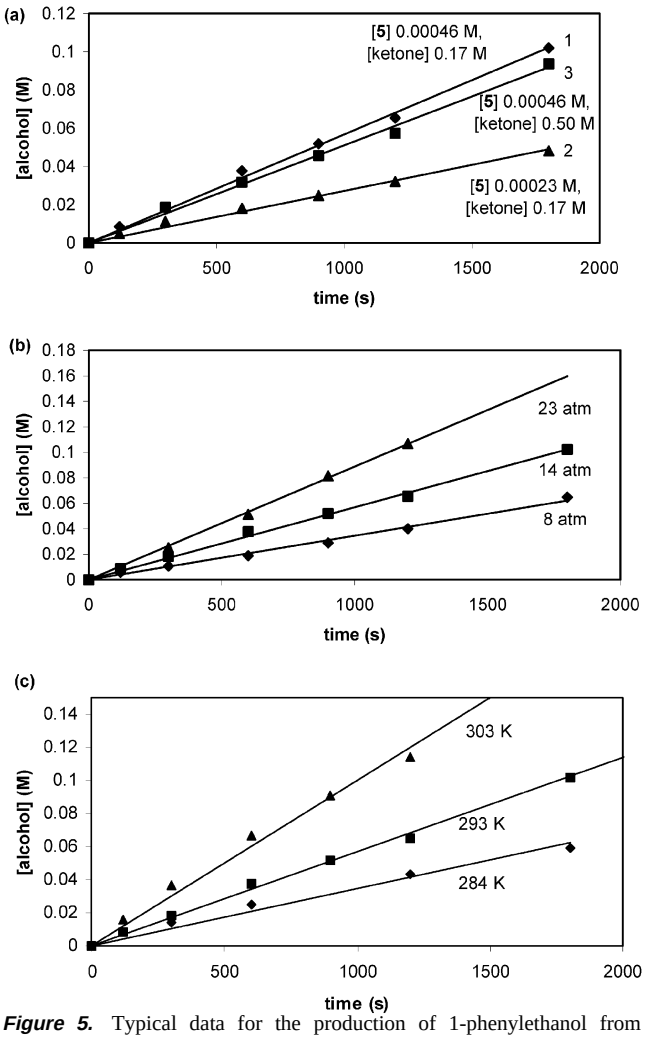

Figure 5. Typical data for the production of 1-phenylethanol from acetophenone in C_6D_6 by use of **5** under 8−23 atm of H_2 (refer to Tables 3 and 4): (a) dependence on catalyst (runs 1, 2) and ketone (runs 1, 3) concentration; (b) dependence on hydrogen pressure (runs 4−6); (c) dependence on temperature (runs 5, 8, 10).

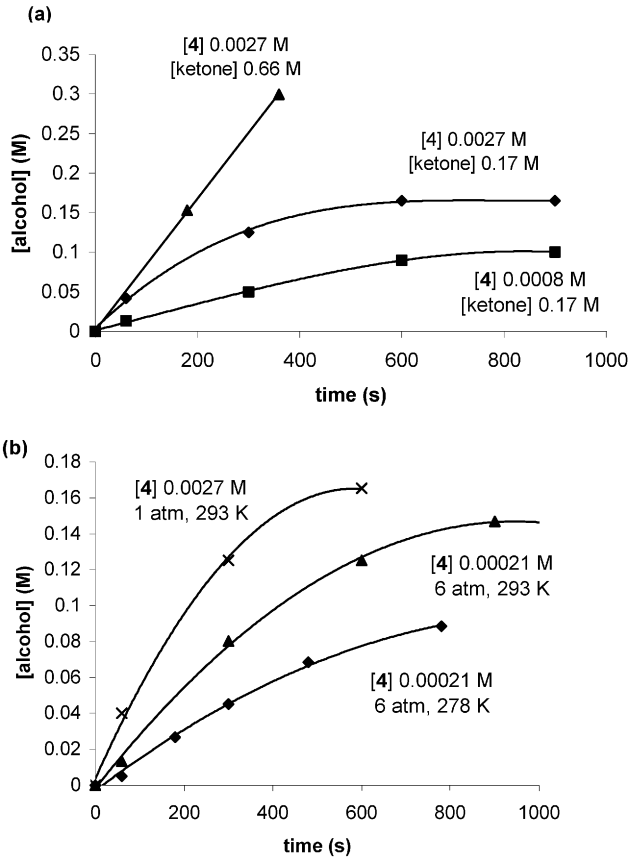

Figure 6. Typical curves for the production of 1-phenylethanol from acetophenone in C_6D_6 by use of **4** under 1 atm of H_2 (refer to Tables 5 and 6): (a) dependence on catalyst (runs 14, 16) and ketone (runs 14, 15) concentration with [**4**] = 0.0027 M except where noted; (b) dependence on pressure (runs 14 and 17, but with different concentrations of **4**) and temperature (runs 17 and 20).

single-crystal X-ray diffraction study of **5**. Of note are the elongated Ru−H bonds of 1.7 Å because of the high *trans* influence of hydride. This elongation relative to normal Ru−H distances of 1.60−1.65 Å accords with the low frequency of the Ru−H vibration of **5** in Nujol (1774 cm^{-1}) and the hydridic reactivity of these hydrides toward carbonyl compounds. Figure 4 also emphasizes the alignment of the axial NH and RuH groups. The main differences in the structures of dihydrides **5** and **6** are the wider P−Ru−P angle of 99.7° and the longer Ru−P distances calculated for the $Ru(PPh_3)_2$ complex compared to those of the Ru(*R*-binap) complex.

Catalysis. Complexes **3**−**6** were found to be active catalysts for the hydrogenation of acetophenone in the neat ketone or preferably in benzene or, less preferably, 2-propanol solutions of the ketone at room temperature and atmospheric hydrogen pressure. $Ru(H)_2$(*R*-binap)(tmen) (**5**) and $RuH(PPh_3)_2(NH_2CMe_2CMe_2NH)$ (**4**) are more stable and were studied in detail. However, even these complexes slowly decompose if left for more than a day in solution under argon, and so fresh catalyst solutions must be used in these studies. Typical conversion curves are plotted in Figures 5 and 6 and analyzed below. Complete and clean conversion of ketone to alcohol is observed for catalyst **5**. The activity of catalyst **4** diminishes with increasing conversion to alcohol but eventually also results in complete, clean conversion to the alcohol. The use of 2-propanol as the solvent resulted in slow transfer hydrogenation of the ketone by the 2-propanol catalyzed by **5** until the reaction mixture was placed under hydrogen gas. The low activity of $RuCl_2$(phosphine)$_2$(diamine) complexes for transfer hydrogenation has been documented previously.[1,42]

The *R*-isomer of 1-phenylethanol is produced in 62−68% ee by use of the chiral catalyst **5**, when benzene is used as the solvent. This ee is relatively independent of the catalyst, ketone, and hydrogen concentrations. The *S*-isomer of 1-phenylethanol is produced in 14% ee when the hydrogenation is done at 3 atm in the neat ketone in the presence of KO^iPr at a ratio of 1500:10:1 = ketone:base:Ru; complete conversion was attained after 48 h. Similarly the *S*-isomer is obtained in 2-propanol without base in 6−14% ee (run 12). Significantly the ee changed to *R* and increased to between 51 and 55% when 2-propanol and excess base were used (run 13).

Kinetics. Reaction rates were monitored by withdrawing samples from the reactor and monitoring the amounts of ketone and alcohol by NMR and GC. Experimental limitations allowed sampling at intervals of about 60 s minimum. The conditions and rate data from the initial linear part of the curves are listed in Tables 3 and 4 for catalyst **5** and Tables 5 and 6 for catalyst **4**.

(42) Pamies, O.; Backvall, J. *Chem. Eur. J.* **2001**, *7*, 5052−5058.

Table 3. Dependence of the Zero-Order Rate of Production of Alcohol on the Concentrations of Catalyst **5** and Ketone[a]

run	[**5**], M	[ketone], M	v_0, zero-order rate, M s^{-1}	$k = v_0/([Ru][H_2])$, M^{-1}s^{-1}
1	4.56×10^{-4}	0.167	5.7×10^{-5}	3.4 ± 0.3
2	2.28×10^{-4}	0.167	2.7×10^{-5}	3.2 ± 0.3
3	4.56×10^{-4}	0.50	5.5×10^{-5}	3.3 ± 0.3

[a] Acetophenone in C_6D_6, 14 atm of H_2 (0.037 M), 293 K.

Table 4. Dependence of the Zero-Order Rate of Production of Alcohol Catalyzed by **5** on the Pressure of H_2 and Temperature and Solvent[a]

run	solvent	pressure of H_2, atm; [H_2], M	temp, °C	v_0, zero-order rate, M s^{-1}	$k = v_0/([Ru][H_2])$, M^{-1}s^{-1}
4	C_6D_6	8; 2.1×10^{-2}	293	3.50×10^{-5}	3.6 ± 0.3
5	C_6D_6	14; 3.7×10^{-2}	293	5.5×10^{-5}	3.4 ± 0.3
6	C_6D_6	23; 6.1×10^{-2}	293	9.0×10^{-5}	3.2 ± 0.3
7	C_6D_6	14, 3.2×10^{-2}	279	2.0×10^{-5}	1.4 ± 0.2
8	C_6D_6	14; 3.3×10^{-2}	284	3.1×10^{-5}	2.1 ± 0.2
9	C_6D_6	14; 3.8×10^{-2}	298	7.5×10^{-5}	4.3 ± 0.2
10	C_6D_6	14; 3.9×10^{-2}	303	9.4×10^{-5}	5.2 ± 0.3
11	C_6D_6[b]	14; 3.7×10^{-2}	293	5.9×10^{-5}	3.5 ± 0.3
12	^{i}PrOH	14; 3.7×10^{-2}	293	1.5×10^{-5}	0.9 ± 0.2
13	^{i}PrOH[b]	14; 3.7×10^{-2}	293	6.4×10^{-5}	3.8 ± 0.3

[a] [**5**] = 4.56×10^{-4} M, [acetophenone] = 0.167 M, solubility of H_2 taken from ref 43. [b] 5 mg of KO^{t}Bu added (KO^{t}Bu:Ru=20:1).

Table 5. Dependence of the Initial Rate of Production of Alcohol on the Concentrations of Catalyst **4** and Ketone[a]

run	[**4**], M	[ketone], M	v_0, initial rate, M s^{-1}	$k = v_0/([Ru][H_2])$, M^{-1}s^{-1}
14	2.7×10^{-3}	0.167	8.0×10^{-4}	111 ± 10
15	2.7×10^{-3}	0.666	8.3×10^{-4}	116 ± 10
16	0.81×10^{-3}	0.167	2.4×10^{-4}	112 ± 10

[a] Acetophenone in C_6D_6; 1.0 atm of H_2 (0.00265 M), 293 K.

Table 6. Dependence of the Initial Rate of Production of Alcohol Catalyzed by **4** on the Pressure of H_2 and Temperature[a]

run	[**4**], M	pressure of H_2, atm; [H_2], M	temp, °C	v_0, initial rate, M s^{-1}	$k = v_0/([Ru][H_2])$, M^{-1}s^{-1}
14	2.7×10^{-3}	1.0; 2.65×10^{-3}	293	8.0×10^{-4}	111 ± 10
17	2.1×10^{-4}	6.0; 1.59×10^{-2}	293	3.9×10^{-4}	115 ± 10
18	2.1×10^{-4}	6.0, 1.48×10^{-2}	286	2.4×10^{-4}	75 ± 5
19	2.7×10^{-4}	6.0, 1.38×10^{-2}	280	2.4×10^{-4}	63 ± 5
20	2.7×10^{-4}	6.0; 1.36×10^{-2}	278	1.9×10^{-4}	52 ± 5

[a] [acetophenone] = 0.166 M.

In the case of **5**, the use of hydrogen pressures of 8−23 atm, catalyst concentrations of less than 10^{-3} M, and ketone concentrations of about 0.2 M usually provided linear kinetic behavior to complete conversion (Figure 5). Therefore, the rates of runs 1−6 are zero order in ketone concentration. The data of Table 3 indicate that, within experimental error, the rate of alcohol production (paralleled exactly by the loss of ketone) is first order in catalyst **5** (runs 1 and 2) and zero order in ketone (runs 1 and 3). A plot of rate/[**5**] versus hydrogen concentration from runs 4−6 of Table 4 yields a straight line with slope 3.3 that passes through the origin.

Therefore, the rate law at 293 K for the range of ketone, catalyst, and H_2 concentrations studied is given by eq 1 where the rate constant for catalyst **5** is $k = 3.3 \pm 0.2$ M^{-1} s^{-1}.

$$\text{rate} = \text{d[alcohol]}/\text{d}t = -\text{d[ketone]}/\text{d}t = k[\mathbf{5}][H_2] \quad (1)$$

Table 7. Activation Parameters

parameter	complex **5**	complex **4**
$\Delta H^{\ddagger}$ (kcal mol^{-1})	8.6 ± 0.5	7.6 ± 0.5
$\Delta S^{\ddagger}$ (cal mol^{-1}K^{-1})	-27 ± 2	-23 ± 2
$\Delta G^{\ddagger}$ (298 K, kcal mol^{-1})	16.6 ± 0.5	14.5 ± 0.5

The data from Table 4 for the temperature dependence of k provides the activation parameters listed in Table 7. The large negative $\Delta S^{\ddagger}$ and the independence of rate on ketone concentration suggest that the addition of dihydrogen to ruthenium is the turn-over limiting step. Table 4 also shows that the rate law for **5** is not affected by added base in benzene (run 11). The activity of **5** when 2-propanol is the solvent (run 12) is less, but the activity can be increased to the level of activity in benzene by the addition of excess potassium *tert*-butoxide (run 13).

The plots of the alcohol concentration versus time for the hydrogenation of acetophenone catalyzed by **4** were usually curved in a single exponential fashion even at low conversions (Figure 6). Therefore, the curves were fitted to single exponentials and the initial rates were evaluated from the differential of the exponential at time zero. The initial rates seem to be independent of the ketone concentration (runs 14, 15), but the rate of hydrogenation slows dramatically with time. Runs 14 and 16 show that the rate is first order in catalyst concentration while runs 14 and 17 provide a first-order dependence on hydrogen concentration. The rate law for catalyst **4** is given by eq 2 with $k = 1.1 \times 10^2$ M^{-1} s^{-1} at 293 K. The approximate activation parameters are listed in Table 7. As with catalyst **5**, the activation of dihydrogen by the amido complex **4** appears to be the turn-over limiting step.

$$\text{rate} = \text{d[alcohol]}/\text{d}t = -\text{d[ketone]}/\text{d}t = k[\mathbf{4}][H_2] \quad (2)$$

The Proposed Mechanism. A likely catalytic cycle for hydrogenation in these systems, similar to the one proposed earlier on the basis of experimental observations, has been derived from computations on the model system {$Ru(PH_3)_2(H)_2$(en) (**6′**) + acetone}, with the results shown in Figures 7 and 8.

In the first step, the *trans* dihydride **6′** forms a weak molecular complex with acetone (the interaction energy shown in Figure 7 is derived from a gas-phase computation; solvation effects would presumably lead to a much weaker interaction). Hydrogenation of acetone is then extremely facile. Incipient bond formation in this early TS (denoted Hydrog. TS in Figures 7 and 8) is signaled by the shortening of the O···H distance (from 2.04 Å to 1.81) in the N−H···O hydrogen bond and of the hydride···carbonyl distance (H···C from 3.03 to 1.78). Small (1−3%) changes, in the expected direction, are observed in other bond lengths. The electronic structure at the transition state reflects the polar nature of this hydrogenation, with NPA partial charges of −0.21 and +0.45, respectively, on the formal hydride and proton species undergoing transfer. The product complex is significantly (6.2 kcal/mol) stabilized by N(amido)···H−O(alcohol) hydrogen bonding.

The next step, the heterolytic splitting of dihydrogen across the formal Ru=N double bond of the amido intermediate **4′**, is predicted to be the slowest in the cycle. This step actually consists of two steps: initial and easy complexation of dihydrogen and then rate-determining proton abstraction by the

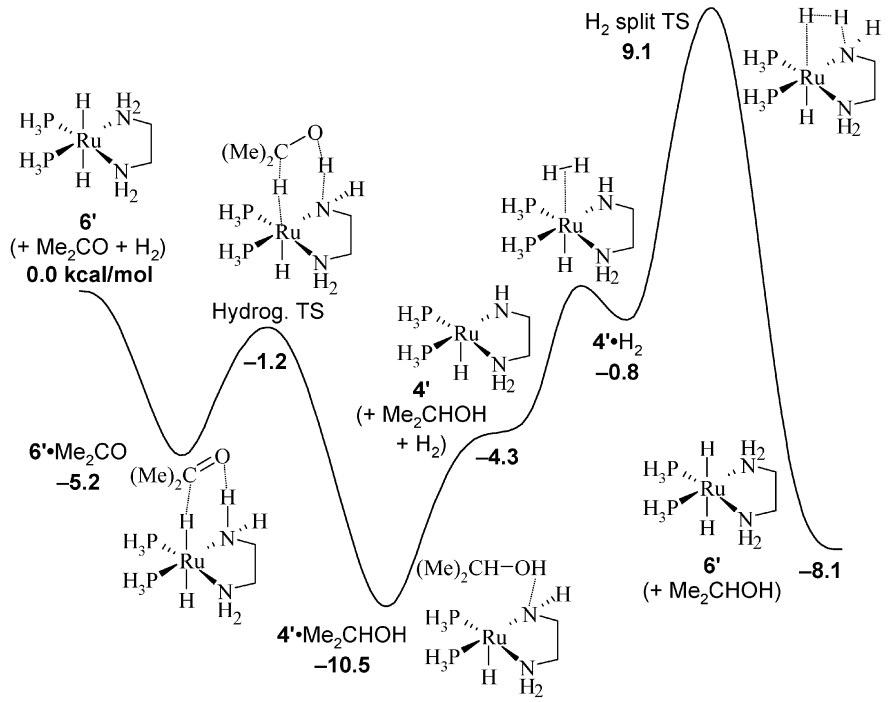

Figure 7. The calculated energetics of the catalytic cycle (in kcal/mol, at the B3LYP/BS B//B3LYP/BS A + zpe level).

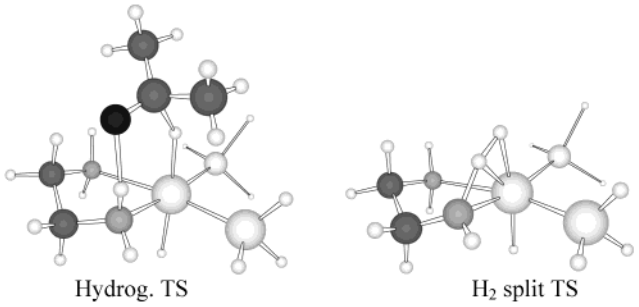

Figure 8. Calculated transition state structures for the reaction of the model dihydride (**6′**) with acetone (Hydrog. TS) and the model amido complex (**4′**) with dihydrogen (H_2 split TS).

amido nitrogen with the transition state denoted "H_2 split TS" in Figures 7 and 8. The dihydrogen complex $Ru(PH_3)_2(H_2)(H)(NHCH_2CH_2NH_2)$ (**4′**·H_2) is rather similar to the initial amido species **4′**, except that the π-bond between the metal and the amido nitrogen has clearly been broken in the presence of the additional ligand, with the Ru−N distance increasing by 0.12 to 2.118 Å and the nitrogen adopting a pyramidalized structure. Accordingly, this addition step is actually *endo*thermic and entropically very unfavorable. Therefore, the dihydrogen complex **4′**·H_2 cannot be expected to be experimentally detectable, as is indeed found. We were unable to locate the transition state for the formation of **4′**·H_2 from **4′** and H_2, but computations confirmed that the barrier involved is very low (<1 kcal/mol above the energy of **4′**·H_2).

The heterolytic nature of the dihydrogen-splitting transition state is confirmed by a calculation of the NPA partial charges on the Ru−H and N−H hydrogens: −0.18 and +0.23, respectively. It is to be noted that the barrier is rather high, at 13.4 kcal/mol relative to the separated amido and dihydrogen reactants, H_2 and **4′**, so that the computations predict this step to be rate-limiting, in agreement with experiment. The overall computed $\Delta S^{\ddagger}$ (from **4′** + H_2 to the TS) is −28.7 cal mol^{-1} K^{-1}, similar to the experimental values of −23 and −28 for catalysis by **4** and **5**, respectively. However, the computed energy barrier of 13.4 kcal/mol is significantly larger than the experimental $\Delta H^{\ddagger}$ values of 7.6 and 8.5 kcal/mol for **4** and **5**, respectively. The origin of this discrepancy is not yet entirely clear, but could be due to a variety of reasons: inaccuracy of the computational method, neglect of solvation effects, the neglect of hydrogen atom tunneling through the barrier, and/or the fact that the barrier height was computed for the small model system instead of the real compound. We have carried out several different calculations of the barrier height and found broadly similar results. Thus, the barrier heights (without zero-point energy correction) do not show a large sensitivity to basis sets (B3LYP/BS A, 14.1 kcal/mol; B3LYP/BS B//B3LYP/BS A, 11.2), or to the density functional used (BP86/BS A, 13.7), or indeed to the inclusion of a continuum description of the benzene solvent(w/ B3LYP/BS A, 13.6). The imaginary frequency at the TS for hydrogen splitting is calculated to be 1312i cm^{-1}, which is compatible with a small degree of tunneling, but probably not enough to account for the experimental activation energy being substantially smaller than the barrier height.

Concerning the accuracy of the model system used, we note that the computed thermochemistry of both of the H_2 addition steps to the amido complexes **3** and **4** to give **5** and **6** (−14.4 and −15.1 kcal/mol, respectively, at the B3LYP/BS C level) is slightly more exothermic than that in the case of the model system, **4′** to **6′** (−11.0 kcal/mol with BS A, without ZPE correction). In terms of the Hammond postulate, this may lead to a slightly earlier and lower barrier, and of course, the electronic and steric effects in the large systems may also affect the barrier height quite independently.

Other Relevant Reactions. Stoichiometric Reactions of the Complexes with Acetophenone. $Ru(H)_2$(*R*-binap)(tmen) or $Ru(H)_2(PPh_3)_2$(tmen) in C_6D_6 react rapidly with 1 equiv of ketone

Scheme 3. Reaction of the Amido Complexes with Acetophenone

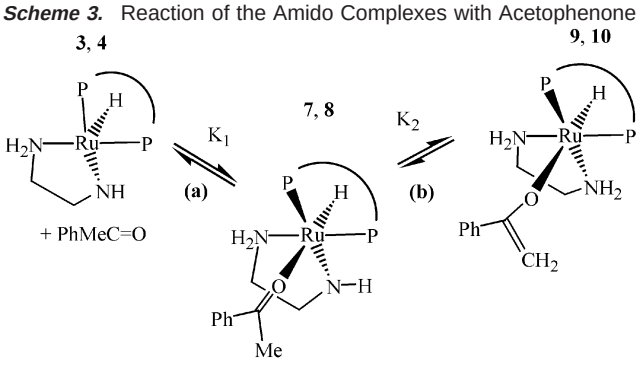

to produce the amido complexes **3** or **4**, respectively, and 1-phenylethanol. The product alcohol weakly and reversibly binds to the amido complexes to cause broadening of the amido NMR signals (see below). This reaction is consistent with the proposed catalytic cycle where the dihydride complexes transfer dihydrogen to the ketone in a low activation energy process (Scheme 1 and Figure 7). When more than 1 equiv of ketone is present, a ketone adduct Ru(*R*-binap)(H)(O=CMePh)(NH_2-CMe_2CMe_2NH) (**7**) or Ru(PPh_3)$_2$(H)(O=CMePh)(NH_2CMe_2-CMe_2NH) (**8**) forms (Scheme 3). The amido complex **3** and free ketone are in rapid equilibrium with **7** with a K_1 (refer to Scheme 3) of approximately 2 M^{-1}. Similarly, **4** and free ketone are in rapid equilibrum with **8** (K_1 0.12 M^{-1}). The broadening and shifting of the hydride resonance of the amido complex **4** toward the chemical shift of the hydride resonance of the ketone adduct **8** is consistent with a rate of greater than 10^3 s^{-1} for the exchange process between complexes **4** and **8**. The ketone adducts reversibly, and more slowly, convert to oxygen-bonded enolate complexes *trans*-Ru(*R*-binap)(H)(OCPh=CH_2)(tmen) (**9**) or Ru(PPh_3)$_2$(H)(OCPh=CH_2)(tmen) (**10**) with a constant K_2 of 20 for the equilibrium between **7** and **9** and K_2 of 10 for that between **8** and **10** (Scheme 3). The enolates are unambiguously identified by the two inequivalent hydrogens on the CH_2 group in the ^{1}H NMR and the characteristic CH_2 and enolate carbon resonances at 168 (CORu) and 79 ppm (CH_2) in the ^{13}C NMR spectra as reported for other oxygen-bonded enolate complexes derived from acetophenone.[44,45] Another supporting feature is the similarity of the hydride and phosphorus chemical shifts to the other alkoxide species **15** and **16** that are described below. The enolate complex **9** along with **7** and **8** can also be independently synthesized by reacting the potassium enolate of acetophenone with complex **1** (eq 3).

$$\text{RuH(Cl)}(R\text{-binap})(\text{tmen}) + \text{K[OCPh=CH}_2] \rightarrow \text{RuH(OCPh=CH}_2)(R\text{-binap})(\text{tmen}) + \text{KCl} \quad (3)$$

The coordination of a sixth ligand such as acetophenone to **3** and **4** is expected to increase the basicity of the amido nitrogen since the lone pair on nitrogen can no longer be stabilized by ruthenium. This leads to the deprotonation of the methyl of the ketone. Similarly, the high basicity of the six-coordinate Ru(II) complex, *trans*-RuH(NH_2)(dmpe)$_2$ (pK^{THF}\{RuH(NH_3)(dmpe)$_2$,fluorenide\}= 31,[16] pK_α^{THF} approximately 40[46]) and its ability to deprotonate CH bonds has been reported.[16] The reactions of Scheme 3 are reversible since reaction of the mixture with dihydrogen produces 1-phenylethanol and the dihydrides **5** and **6** via the amido complexes **3** and **4**.

Scheme 4. Decomposition of the Catalyst Systems by Reaction with Excess Ketone under Ar

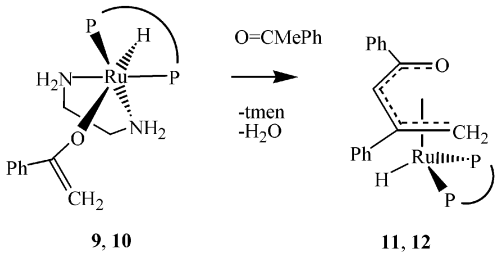

The catalysts **4** and **5** will decompose if they are left for extended periods of time in the presence of high concentrations of ketone under Ar. An aldol condensation reaction involving the enolate complexes **9** or **10** and elimination of water produces, after loss of the tmen ligand, the new complexes Ru(*R*-binap)H(η^5-$CH_2CPhCHCPhO$) (**11**) or Ru(PPh_3)$_2$H(η^5-$CH_2CPhCHCPhO$) (**12**) (Scheme 4) that contain η^5-allyl ketone ligands. The X-ray structure of the *R*-binap complex **11** is shown in Figure 9. The hydride was not located in the structure, but a solution of some crystals displayed the expected hydride resonance. It could be positioned *trans* to the oxygen where there is an open site on the ruthenium in the structure. The activation of coordinated enolate to form aldol condensation products is well documented in the literature.[44] Mesityl oxide is known to bond in a similar η^5-fashion in Ru(C_5Me_5)(η^5-$CH_2CMeCHC(O)Me$).[47]

Stoichiometric Reactions of the Complexes with Alcohols. When 20 equiv of 1-phenylethanol is added to amido complex **4** in C_6D_6, the color lightens from orange to yellow-green and the hydride resonance broadens and shifts from −21.1 ppm to lower field (−18.7 ppm) due to fast exchange between **4** and free alcohol and a complex of the alcohol RuH(OHCHMePh)(PPh_3)$_2$($NH_2CMe_2CMe_2NH$) (**14a**) as shown in step (a) of Scheme 5. The structure of the alcohol adduct is unknown but could be either oxygen-bonded to ruthenium or hydrogen-bonded to the amido nitrogen as in step (b) of Scheme 5. The latter structure is like the 2-propanol adduct with **4′** shown in Figure 7. The chemical shift of the hydride of **14a** must be less than −18.7 ppm in order to average with that of **4** to produce the observed peak at −18.7. The hydrogen-bonded structure was

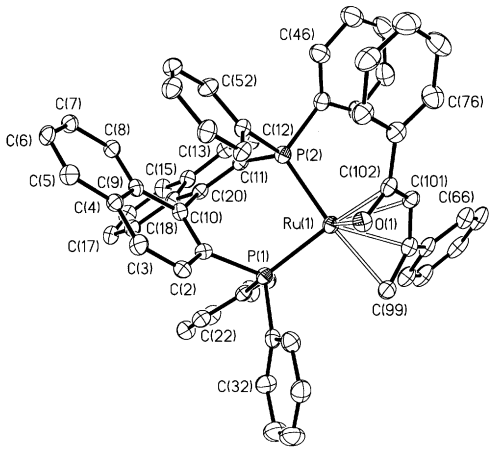

Figure 9. The molecular structure of *trans*- RuH(*R*-binap)(η^5-$CH_2C(Ph)CHC(O)(Ph)$) (**11**).

(43) *Solubility Data Series, Hydrogen and Deuterium*, *5/6*; Young, C. L., Ed., Pergamon Press: New York, 1981.
(44) Solari, G.; Solari, E.; Floriani, C. *Organometallics* **1997**, *16*, 508−510.
(45) Culkin, D. A.; Hartwig, J. F. *J. Am. Chem. Soc.* **2001**, *123*, 5816−5817.

Scheme 5. Reaction of the Amido Complexes with 1-Phenylethanol

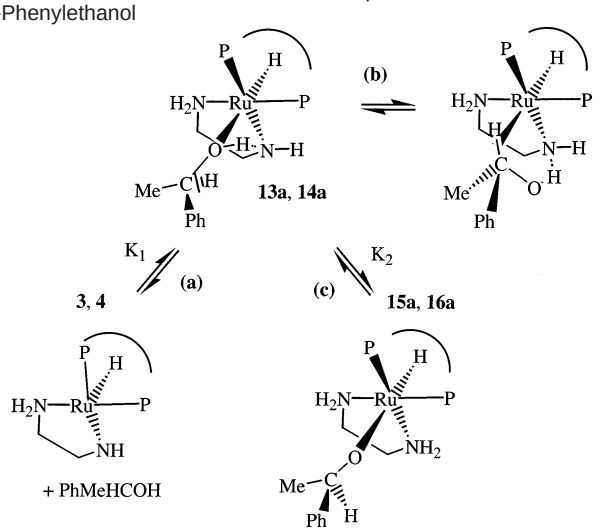

calculated to be a stable one as indicated above (Figure 7), but the NMR behavior is similar to that of the *tert*-butyl alcohol complex **14b** that is more likely to have the alcohol oxygen-bonded to ruthenium (see below). This rapidly exchanging system is in a slower 1:1 equilibrium (Scheme 5, step (c)) with the alkoxide complex RuH(OCHMePh)(PPh_3)$_2$(tmen) **16a**. This is identified by its triplet hydride resonance at −18.6 ppm and singlet at 69.9 ppm in the $^{31}P\{^1H\}$ NMR spectrum. The protonation of amido complexes by alcohols to give alkoxide complexes and amines has been reported.[15]

The addition of 5 equiv of *tert*-butyl alcohol to **4** results in a similar color change, broadening of the amido resonances, and shifting of the hydride to −18.7 ppm as a result of the formation of the alcohol adduct **14b**. However, much less of the alkoxide species *trans*-RuH(O^{t}Bu)(PPh_3)$_2$(tmen) **16c** is produced (hydride triplet at −17.7 ppm, J_{PH} 25.5 Hz, ^{31}P at 70.3 ppm). This is consistent with the more acidic alcohol 1-phenylethanol pushing the equilibrium (c) of Scheme 5 farther to the alkoxide complex **16a** than does the less acidic alcohol, *tert*-butyl alcohol. 2-Propanol shows similar behavior toward **4** as *tert*-butyl alcohol but small amounts of Ru(H)$_2$(PPh_3)$_2$(tmen) are also produced by a β-hydride elimination reaction.

Ru(H)$_2$(*R*-binap)(tmen) reacts with 90% ee (*S*)-1-phenylethanol to produce an equilibrium mixture of two diastereomeric alkoxide complexes RuH(OCHPhMe)(*R*-binap)(tmen) **15a** along with the suspected but undetected intermediates containing nonclassical RuH···HO and Ru(H_2)···O hydrogen bonds via the mechanism proposed in Scheme 6. The alkoxide complexes are identified by hydride resonances at −17.0 and −17.1 ppm and two doublets for each diastereomer in the ^{31}P NMR. The intermediate species shown in Scheme 6 are in fast exchange with the dihydride **5** as suggested by the broadening ($w_{1/2}$ 50 Hz at 300 MHz) of the hydride resonance of **5** at −4.8 ppm when alcohol is added. The hydrides of **5** can act as hydrogen bond acceptors from the alcohol donor to form hydridic-protonic bonds.[25−27,40,48−52] Reaction (a) of Scheme 6 could lead to a

Scheme 6. Reaction of the Dihydrides with Alcohols

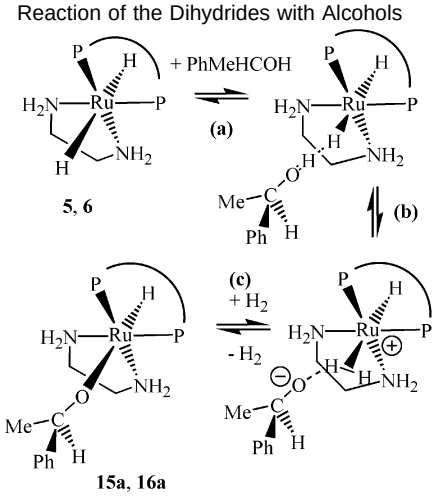

broadening of the hydride resonance of **5** by exchange and T_1 shortening as observed for the closely related system of *trans*-RuH_2(dppm)$_2$ reacting with phenol.[53] A rapid exchange of **5** with the ion-paired dihydrogen complex of Scheme 6 may also be responsible for the broadening of the hydride resonance because the chemical shift of the dihydrogen resonance is likely to be different from that of **5** and the T_1 of a dihydrogen ligand in such *trans*-HRu(H_2) complexes are very short.[54] The alkoxide of the ion pair may accept a nonclassical hydrogen bond from the Ru(H_2) moiety by analogy to the fluoride of BF_4^- in the observed Os(H_2)···FBF_3 hydrogen bond.[55] The reactions of Scheme 6 are reversed to the dihydride by reaction with 1 atm of H_2. There is a report of a similar reactivity of a methoxide ion pair that is postulated to form from *mer*-IrH(OMe)(Ph)-(PMe_3)$_3$.[56]

2-Propanol is often used as the solvent for ketone hydrogenation catalyzed by Noyori catalysts, and bases such as potassium *tert*-butoxide are usually added to activate the dichloride precatalyst. This alcohol reacts with Ru(H)$_2$(*R*-binap)(tmen) under Ar according to Scheme 6 to produce more of the isopropoxide complex *trans*-RuH(^{i}PrO)(*R*-binap)(tmen) **15c** and dihydrogen as the ratio of the amount of 2-propanol to benzene increases. The isopropoxide complex is identified by a triplet in the hydride region at −17.5 ppm and two doublets for inequivalent phosphorus nuclei in the ^{31}P NMR spectrum. The addition of an excess of KO^{t}Bu causes the partial regeneration of dihydride **5**, presumably by reducing the acidity of the alcohol mixture so that the amido complex **3** is produced as in Scheme 5 and this then reacts with dihydrogen present in the solution to give back **5**.

Stoichiometric Reactions of the Complexes with Formic Acid. Ru(H)$_2$(*R*-binap)(tmen) and RuH(PPh_3)$_2$($NH_2CMe_2CMe_2$-NH) react with 1 equiv of formic acid to produce the formate

(46) Abdur-Rashid, K.; Fong, T. P.; Greaves, B.; Gusev, D. G.; Hinman, J. G.; Landau, S. E.; Morris, R. H. *J. Am. Chem. Soc.* **2000**, *122*, 9155−9171.
(47) Navarro, M. E.; Chazaro, L. F.; Gonzalez, F. J.; Paz-Sandoval, M. A. *J. Electroanal. Chem.* **2000**, *480*, 18−25.
(48) Bakhmutov, V. I.; Bakhmutova, E. V.; Belkova, N. V.; Bianchini, C.; Epstein, L. M.; Masi, D.; Peruzzini, M.; Shubina, E. S.; Vorontsov, E. V.; Zanobini, F. *Can. J. Chem.* **2001**, *79*, 479−489.
(49) Belkova, N. V.; Ionidis, A. V.; Epstein, L. M.; Shubina, E. S.; Gruendemann, S.; Golubev, N. S.; Limbach, H. H. *Eur. J. Inorg. Chem.* **2001**, 1753−1761.
(50) Messmer, A.; Jacobsen, H.; Berke, H. *Chem. Eur. J.* **1999**, *5*, 3341−3349.
(51) Custelcean, R.; Jackson, J. E. *Chem. Rev.* **2001**, *101*, 1963−1980.
(52) Belkova, N. V.; Shubina, E. S.; Ionidis, A. V.; Epstein, L. M.; Jacobsen, H.; Messmer, A.; Berke, H. *Inorg. Chem.* **1997**, *36*, 1522−1525.
(53) Ayllon, J. A.; Gervaux, C.; Sabo-Etienne, S.; Chaudret, B. *Organometallics* **1997**, *16*, 2000−2002.
(54) Bautista, M. T.; Cappellani, E. P.; Drouin, S. D.; Morris, R. H.; Schweitzer, C. T.; Sella, A.; Zubkowski, J. *J. Am. Chem. Soc.* **1991**, *113*, 4876−4887.
(55) Schlaf, M.; Lough, A. J.; Maltby, P. A.; Morris, R. H. *Organometallics* **1996**, *15*, 2270−2278.
(56) Blum, O.; Milstein, D. *J. Organomet. Chem.* **2000**, *593−594*, 479−484.

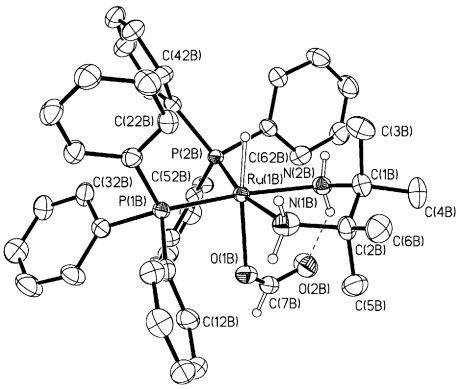

Figure 10. The molecular structure of *trans*-Ru(PPh_3)$_2$(H)(tmen)(OCHO) (**18**).

Chart 2. The Similarity in the Structure of the Formate Complexes and the Models of the Proposed Transition State for the Transfer of Dihydrogen to the Ketone

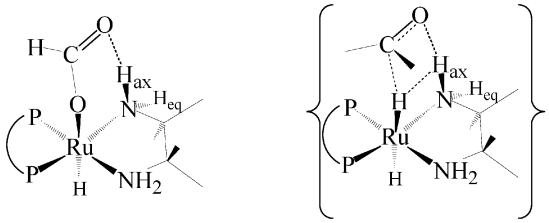

complexes *trans*-Ru(*R*-binap)(H)(tmen)(OCHO) (**17**) and *trans*-Ru(PPh_3)$_2$(H)(tmen)(OCHO) (**18**), respectively. The structure of **18** as determined by single-crystal X-ray diffraction is shown in Figure 10. The carbonyl of the formate is seen to be hydrogen-bonded to an axial NH of the tmen ligand. There is a marked similarity to the transition state for the transfer of H(δ^-) and H(δ^+) equivalents to the ketone shown in Scheme 1 and Figure 8 (Chart 2). The computed structure for this formate complex is very similar. The complex [(OHCO)$(NH_3)_4$RuORu$(NH_3)_4$(OCHO)]Cl_3 has similar hydrogen-bonded formate groups.[57]

Discussion

The current work provides convenient routes to well-defined unprecedented hydridoamido complexes {RuP_2}(H)($NH_2CMe_2CMe_2NH$) and dihydridediamine complexes *trans*-{RuP_2}$(H)_2$(tmen) for use in probing the mechanism of the catalytic hydrogenation of ketones. The structure determination of the distorted trigonal bipyramidal amido complex **4** is particularly significant because it is this species that activates dihydrogen in the turn-over limiting step. This has led to a better understanding of the catalytic cycle shown in Scheme 1 as well as new additions to the scheme reflecting the possible side reactions of the catalytic intermediates with the reactant ketone and the product alcohol (Scheme 7). In particular, high ketone concentrations may lead to the formation of enolates **9** or **10** and high alcohol concentrations may lead to the formation of alkoxide complexes **15** or **16**. These equilibria are reversible, and the extent of formation of these species appears to be a function of the dihydrogen pressure. We have shown that all of the side equilibria are reversed back to the dihydride under 1 atm of H_2. However, the operation of side reactions could explain the more complex kinetic behavior of the hydrogenation of acetophenone catalyzed by **4** or **5** at 1 atm of H_2 under certain conditions. Clearly there must be competition between dihydrogen and these organics for reaction with ruthenium. A further investigation of the reaction rates of individual steps in the cycle, a wider range of ketone and catalyst concentrations, and deuterium isotopic labeling and rate studies are needed before a complete understanding of these fairly complex systems is obtained.

Heterolytic Splitting of Dihydrogen. The negative entropy of activation observed experimentally and calculated for the model system demonstrates the loss of entropy of dissolved dihydrogen on forming the Ru(HH)N transition state in the turnover limiting step. The activation parameters of Table 7 are similar to those for the oxidative addition of dihydrogen to rhodium(I) complexes [Rh(mac)(dipamp)]$^+$ ($\Delta H^‡$ 7.5 kcal/mol, $\Delta S^‡$ −21 cal mol^{-1} K^{-1} for the minor diastereomer and $\Delta H^‡$ 10.7 kcal/mol, $\Delta S^‡$ −23 cal mol^{-1} K^{-1} for the major diastereomer)[58] and to a rutheniumcluster (μ-H)$_2$Ru$_3$(CO)$_8$(μ-P(^{t}Bu)$_2$)$_2$ ($\Delta H^‡$ 8.4 kcal/mol, $\Delta S^‡$ −37.8 cal mol^{-1} K^{-1}).[59] The enthalpies of activation of Table 7 of 8.6 and 7.6 kcal mol^{-1} are smaller than that calculated (13.4) for the model system. The observation that the dihydrides under Ar lose dihydrogen (with heating for complex **5**) to give the amido complexes also suggests that there is only a moderate barrier to dihydrogen addition/loss. This reversible heterolytic splitting of dihydrogen at the Ru═N bond of the amido complexes is an unprecedented feature of these systems. The amido nitrogen in the six-coordinate intermediate {Ru}(H)(H_2)($NHCMe_2CMe_2NH_2$) acts as a powerful base in this heterolytic activation process. The basicity of the amido nitrogen in **3** or **4** is apparent from the reactions of Schemes 3 and 5 where both a ketone and an alcohol are deprotonated by this nitrogen.

Hydride and Proton Transfer to the Ketone. Our study suggests that the *trans*-dihydride species transfer hydride and proton equivalents to the ketone rapidly and in a concerted fashion with a very low calculated activation barrier (4 kcal mol^{-1}). This is the enantioselective step of the reaction when a chiral ligand like *R*-binap is present. The model proposed previously to explain the enantioselectivity of Noyori-type RuXY(diamine)(binap) catalysts[9] nicely accounts for the current observation of *R*-alcohol being produced in benzene solution. Usually *S*-alcohol is produced in the Noyori systems with *R*-binap and chiral *R,R*-diamines that are locked in the λ conformation as discussed previously.[9] The favored conformation of the five-membered ring formed by the tmen ligand in **5** is δ instead of λ on the basis of evidence from its crystal structure and the observation of four inequivalent tmen CH_3 resonances in the ^{1}H NMR spectrum. Therefore, the ketone would be favored to approach complex **5** as indicated in Chart 3. The oxygen will start forming a hydrogen bond with the axial NH while the phenyl group avoids the bulky *R*-binap backbone. Since **5** is C_2 symmetric, the asymmetric induction will be identical for $H^{\delta+}/H^{\delta-}$ transfer from the $HRuNH_{ax}$ unit on either face of the complex. The fact that (*S*)-1-phenylethanol is produced in low ee under other conditions (neat ketone, 2-propanol) probably indicates that side reactions are interfering with the true enantioselectivity of the system. For example, the mixture of diastereomeric alkoxide complexes RuH(OCHPh-

(57) Emerson, J.; Clarke, M. J.; Ying, W.-L.; Sanadi, D. R. *J. Am. Chem. Soc.* **1993**, *115*, 11799−11805.

(58) Landis, C. R.; Halpern, J. *J. Am. Chem. Soc.* **1987**, *109*, 1746−1754.

(59) Safarowic, F. J.; Bierdeman, D. J.; Keister, J. B. *J. Am. Chem. Soc* **1996**, *118*, 11805−11812.

Scheme 7

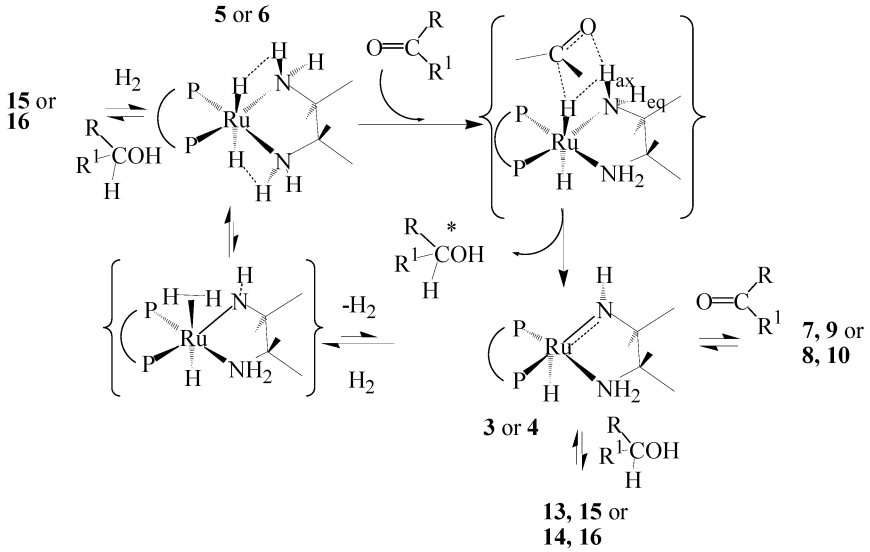

Chart 3. Stereochemical Model To Explain the Enantioselectivity of the Transfer of Dihydrogen to the Ketone from Complex **5**

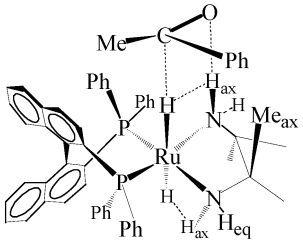

Me)(*R*-binap)(tmen) might also be poorer hydrogenation catalysts that produce the alcohol in low ee. When base is added to the 2-propanol solution of **5** under H_2, the inherent enantioselectively of the dihydride **5** is reestablished in the catalytic hydrogenation of acetophenone (51−55% ee (*R*)-phenylethanol in 2-propanol with base vs 58−68% ee *R* in benzene).

Our mechanism indicates that the amido and dihydride intermediates are key to catalytic activity. The build up of the acidic alcohol 1-phenylethanol from the hydrogenation of acetophenone in the presence of high concentrations of **4** seems to result in catalyst deactivation by alkoxide formation (Schemes 5 and 6) as the reaction proceeds, and this could explain the curved plots of Figure 6. The formation of less active or inactive alkoxide species when 2-propanol is used as the solvent for **5** could explain its reduced activity in this solvent compared to benzene. The much lower dielectric constant of benzene (<5) compared to that of 2-propanol (approximately 18) means that alcohols in these two solvents will have greatly different acidities. For example, cyclohexanol has a pK_α^{THF} of about 38 in THF (dielectric constant 7.4)[46] but near 18 in the neat alcohol (dielectric constant 15). The much poorer basicity of benzene compared to 2-propanol is also a factor. The addition of excess potassium *tert*-butoxide to 2-propanol solutions of **5** restores the catalytic activity to the level of the amido/dihydride mixture in benzene possibly by reducing the Brønsted acidity of the solution so that the equilibria of Schemes 5 and 6 are reversed back to the active amido (and dihydride by reaction with H_2). A future complete kinetic analysis in 2-propanol would have to account for this base concentration dependence.

The addition of potassium *tert*-butoxide to a ketone solution in benzene does not affect the rate of catalysis; therefore there is no "potassium effect"[8] in this case. A role for potassium ions in the Noyori $RuCl_2$(diamine)(diphosphine)/KOR/H_2/i-PrOH catalyst systems could be to precipitate chloride during hydride formation as has already been observed for related reactions with alkali metal ions. The role of sodium ion in forming hydridochloroiron-group complexes from dichlorocomplexes under dihydrogen by precipitating NaCl has been clearly demonstrated.[54,60−62] Sodium ions and a strong base are also effective reagents to convert hydridochloroiron-group complexes to *cis*-[54,60,62] and *trans*-[61] dihydridocomplexes under 1 atm of dihydrogen. We have shown that the dihydrides $\{RuP_2\}H_2$-(diamine) are the active catalysts for the hydrogenation of neat ketone in the absence of a base while the hydridochloro complexes $\{RuP_2\}$H(Cl)(diamine) are inactive unless activated by potassium selectride or potassium alkoxide under H_2.[5,24] Similarly, the dihydride $RuH_2(PPh_3)_3$ is the active catalyst in the hydrogenation of ketones by transfer of dihydrogen from the alcohol solvent; it is formed by treating the inactive catalyst $RuHCl(PPh_3)_3$ with NaOH/^{i}PrOH.[63]

Conclusions

The use of a diamine without α-hydrogens allows the isolation of well-defined and well-behaved *trans*-dihydrides and hydridoamido complexes so that mechanistic details of the hydrogenation of ketones catalyzed by Noyori-like (diamine)-(phosphine)ruthenium complexes can be examined. The results are consistent with the cycle of Scheme 1 with heterolytic splitting of dihydrogen across the polar ruthenium−nitrogen bond as the turn-over limiting step under the reaction conditions that we have examined. The structure of chiral dihydrides is important because this determines the enantioselectivity of the hydrogenation of prochiral ketones. A transition state for the polar hydrogenation reaction of Chart 3 explains the favored production of (*R*)-1-phenylethanol by $Ru(H)_2$(*R*-binap)(tmen) in benzene or 2-propanol with base. $Ru(H)_2$(*R*-binap)(tmen)

(60) Cappellani, E. P.; Maltby, P. A.; Morris, R. H.; Schweitzer, C. T.; Steele, M. R. *Inorg. Chem.* **1989**, *28*, 4437−4438.
(61) Bautista, M. T.; Earl, K. A.; Maltby, P. A.; Morris, R. H.; Schweitzer, C. T. *Can. J. Chem.* **1994**, *72*, 547−560.
(62) Earl, K. A.; Jia, G.; Maltby, P. A.; Morris, R. H. *J. Am. Chem. Soc.* **1991**, *113*, 3027−3039.
(63) Aranyos, A.; Csjernyik, G.; Szabo, K. J.; Backvall, J. E. *Chem. Commun.* **1999**, 351−352.

contains a chiral diphosphine along with an achiral diamine and yet yields the product in moderate ee under our catalytic conditions. The Noyori systems that produce the alcohol in high ee contain a diamine with a chirality that is matched with that of the chiral diphosphine ligand.[1,2] Calculations support the mechanistic proposal. While calculations have been carried out on the step for Ru-H/N-H hydrogen transfer to the ketone for other catalysts,[2,6] our theoretical treatment of the heterolytic splitting of dihydrogen at the amido complex is novel. We have obtained a better understanding of the effect of the side reactions involving the reactant ketone and the product alcohol and the effect of the solvent on the acidity of the alcohol and its subsequent reactions with the active catalyst species, the hydridoamido and the dihydrido(diamine) ruthenium(II) complexes. The novel amido complexes display an interesting reactivity with weak acids (either dihydrogen, alcohol, or acetophenone). Coordination of the acid causes the loss of Ru═N double bond character and pyramidalization of the amido nitrogen as the complex changes from five- to six-coordinate. This serves to increase the basicity of the amido nitrogen and, at the same time, the acidity of the H_2, alcohol, or ketone ligand by the effect of the Lewis acidic ruthenium center. This dual effect favors the proton transfer from the weakly acidic H_2 or alcohol hydroxyl or ketone methyl to the amido nitrogen.

Experimental Section

General. All preparations and manipulations were carried out under hydrogen, nitrogen, or argon atmospheres with the use of standard Schlenk, vacuum line, and glovebox techniques in dry, oxygen-free solvents. Tetrahydrofuran (THF), diethyl ether (Et_2O), and hexanes were dried and distilled from sodium benzophenone ketyl. Deuterated solvents were degassed and dried over activated molecular sieves. Potassium tri-*sec*-butylborohydride and potassium *tert*-butoxide were supplied by Aldrich Chemical Co. Complexes **1**, **3**, and **5** were prepared and characterized as described previously.[9] NMR spectra were recorded on a Varian Unity-500 (500 MHz for ^{1}H), a Varian Unity-400 (400 MHz for ^{1}H), or a Varian Gemini 300 MHz spectrometer (300 MHz for ^{1}H and 121.5 for ^{31}P). All ^{31}P chemical shifts were measured relative to 85% H_3PO_4 as an external reference. ^{1}H chemical shifts were measured relative to partially deuterated solvent peaks but are reported relative to tetramethylsilane. ^{1}H NMR T_1 measurements were carried out at 500 MHz using the inversion−recovery method. The temperature of the probe was calibrated using the temperature dependence of the chemical shifts of MeOH. ^{1}H NMR NOE, NOESY, ROESY, COSY, and CIGAR experiments were also carried out at 500 MHz. 1-Phenylethanol obtained from the catalytic hydrogenation of acetophenone was characterized by its ^{1}H and ^{13}C NMR spectra. All infrared spectra were obtained on a Nicolet 550 Magna-IR spectrometer. Microanalyses were performed by Guelph Chemical Laboratories Ltd. or at the University of Toronto. Gas chromatography was carried out on a Perkin-Elmer Autosystem XL with a Chrompack capillary column (Chirasil-Dex CB 25 m × 0.25 mm) utilizing an H_2 carrier gas at a column pressure of 5 psi, an oven temperature of 130 °C, an injector temperature of 250 °C, and an FID of 275 °C. The retention times were acetophenone 5.0 min, (*R*)-1-phenylethanol 8.5 min, (*S*)-1-phenylethanol 9.1 min.

X-ray Structure Analysis. Crystals were obtained by the slow diffusion of either diethyl ether or hexanes into THF or benzene solutions of the desired compounds under an argon atmosphere. Data were collected on a Nonius Kappa-CCD diffractometer using Mo Kα radiation (λ = 0.710 73 Å). The CCD data were integrated and scaled using the DENZO-SMN software package, and the structures were solved and refined using SHELXTL V5.0. Wherever reported, hydrides were located and refined with isotropic thermal parameters.

RuHCl(PPh$_3$)$_2$(tmen), 2. Under N_2, 2,3-diamino-2,3,-dimethylbutane (390 mg, 3.36 mmol) was stirred into a purple suspension of RuHCl(PPh$_3$)$_3$ (2.001 g, 2.165 mmol) in THF (5 mL). Over a 20 min period, there was a gradual color change to yellow along with the precipitation of a black solid. The black precipitate was filtered. A bright yellow solid precipitated out of the filtrate upon the addition of an equal volume of hexanes. The solid was filtered and washed with one 3 mL portion of 5:1 hexanes:THF and one 3 mL portion of hexanes. The solid was dried under vacuum. A concentrated solution of the yellow solid in THF was layered with hexanes in an NMR tube. The crystals that formed were used to obtain an X-ray crystal structure. Yield: 1.27 g (76%). Anal. Obsd: C, 64.83; H, 6.45; N, 3.49. Calcd: C, 64.81; H, 6.09; N, 3.60.^{1}H NMR (CD_2Cl_2) δ: 7.0−7.5 (m, phenyl), 2.7 (d, NH), 1.8 (d, NH), 1.0 (2 overlapping singlets, CH_3), −18.5 (t, J_{H-P} = 26 Hz, RuH). ^{31}P{^{1}H} NMR (CD_2Cl_2): δ 69.8 (s, RuP). IR (Nujol): 3337, 3323, 3278, 3241 cm^{-1}(NH), 2011 (RuH).

RuH(PPh$_3$)$_2$(NH$_2$CMe$_2$CMe$_2$NH), 4. (a) A yellow solution of **2** (600 mg, 0.771 mmol) in THF (3 mL) was made under Ar. A K-Selectride solution (851 mg of a 1 M THF solution, 0.932 mmol), diluted in THF (1.5 mL), was slowly added to the solution of **2** with stirring. An immediate color change from yellow to red was observed. This was stirred for 2 h and then left static for 48 h. The solution was evaporated under vacuum. The resulting orange solid was extracted from the residue with ether, and the extracts were filtered. The filtrate was evaporated under vacuum, leaving an orange solid. The solid was stirred in hexanes and then filtered, washed with diethyl ether, and dried in a vacuum. Yield: 303 mg (53%). (**b**) Potassium *tert*-butoxide (0.58 g, 5.2 mmol) was slowly added to a solution of **2** (2.7 g, 3.5 mmol) in 10 mL of THF to give an orange solution. This was stirred for 2 h and then filtered and washed. The filtrate was evaporated to dryness, and the residue was stirred with hexanes to produce an orange solid that was filtered and washed with diethyl ether and dried in a vacuum (2.4 g, 94%). A concentrated solution in benzene was layered with hexanes in an NMR tube. The crystals that formed were used to obtain an X-ray crystal structure. ^{1}H NMR (C_6D_6) δ: 7.7 (s, broad, phenyl), 6.9−7.0 (m, phenyl), 3.5 (s, N−H), 3.4 (s, N−H), 1.0 (s, C−H), 0.7 (s, C−H), −21.1 (t, J_{H-P} = 36 Hz, Ru−H). ^{31}P NMR (C_6D_6) δ: 72.4 (s, Ru−P). IR(Nujol): 1896 cm^{-1} (νRuH), 3331, 3277, 3136 cm^{-1} (νNH). Several attempts at elemental analysis failed because of the air and nitrogen sensitivity of the sample.

***trans*-RuH$_2$(PPh$_3$)$_2$(tmen), 6.** This complex was observed by reacting **4** in C_6D_6 with 1 atm of H_2. ^{1}H NMR (C_6D_6) δ: 6.7−8.0 (m, phenyl), 2.2 (s, NH), 0.6 (s, CH_3), −5.5 (t, J_{H-P} = 18 Hz, Ru−H). ^{31}P{^{1}H} NMR (C_6D_6) δ: 87.8 (s, Ru−P), 58.8 (s, weak, decomposition product $RuH_4(PPh_3)_3$).

Reaction of 5 with Acetophenone. The addition of excess acetophenone (10−50 mg) to a solution of **5** (30 mg) in C_6D_6 (0.5 g) resulted in the formation of 1-phenylethanol and an equilibrium mixture of **3** and a ketone adduct, **7**, in rapid exchange, along with the enolate complex RuH(OC(Ph)═CH$_2$)(*R*-binap)(tmen) (**9**) in slow exchange. NOESY, ROESY, COSY, and CIGAR experiments were used to determine the structure of **9**. ^{1}H NMR(C_6D_6) for **9**. δ: −17.96 (dd, $^2J_{HP}$ = 25.2, 25.0 Hz, 1H, RuH), 0.481 (s, 3 H, Me), 0.516 (s, 3 H, Me), 0.604 (s, 3 H, Me), 0.700 (s, 3 H, Me), 1.39 (d, $^2J_{HH}$ = 9.9 Hz, 1H, NH), 2.44 (d, $^2J_{HH}$ = 9.9 Hz, 1H, NH), 3.42 (d, $^2J_{HH}$ = 9.9 Hz, 1H, NH), 4.86 (d, $^2J_{HH}$ = 9.9 Hz, 1H, NH), 3.21 (s, 1H CH_2), 4.54 (s, 1H CH_2), 6.22−8.88 (m, 32 H). ^{13}C{^{1}H} NMR δ: 168 (CORu), 79 (CH_2), 25.9, 26.2, 26.5, 27.2 (CH_3 of tmen). ^{31}P{^{1}H} δ: 68.4 (d), 69.4 (d), $^2J_{PP}$ = 45.3 Hz.

The equilibrium constant for the reaction of **3** with acetophenone was obtained as follows: To 41 mg of **5** in 550 mg of C_6D_6 was added cumulative aliquots of 10, 20, 30, and 41 mg of acetophenone. The concentrations of acetophenone, **3**/**7**, and **9** were obtained from ^{1}H and ^{31}P{^{1}H} NMR measurements (see Supporting Information).

Reaction of 1 with KOC(Ph)(CH$_2$). A 10 mg sample of KOC(Ph)(CH$_2$) (prepared from the reaction of KH with acetophenone) was

added to a solution of **1** (50 mg, 0.049 mmol) in C_6D_6 (0.6 g) in an NMR tube and the mixture shaken vigorously for 2 h. The ^{1}H NMR and ^{31}P{^{1}H} NMR spectra show the presence of **1** (29%), **3** (35%), and the enolate complex **9** (36%). The ^{1}H NMR spectrum also shows the presence of acetophenone.

Reaction of 4 with Acetophenone. The reaction of excess acetophenone with a solution of **4** (31 mg in 0.7 mg C_6D_6) resulted in an equilibrium mixture of the enolate complex RuH(OC(Ph)(CH_2)(PPh_3)$_2$-(tmen) (**10**) along with free ketone in fast exchange with **4** and the ketone adduct **8**. When left for greater than 48 h, the aldol condensation product RuH(PPh_3)$_2$(η^5-CH_2CPhCH_2CPhO) (**12**) is formed (see below). ^{1}H NMR for **10**. δ: −19.4 (t, J_{H-P} = 25.5 Hz, 1H, RuH), 0.62 (s, 6H, CH_3), 0.71 (s, 6H, CH_3), 3.76 (s, 1H, CH), 3.8 (s, 1H, CH), 2.6 (br, 4H, NH), 6.8−7.9 (m, 35H, phenyl). ^{31}P{^{1}H} δ: 67.1 (s).

The equilibrium constant for the reaction of **4** with acetophenone was obtained as follows: To 31 mg of **4** in 697 mg of C_6D_6 was added cumulative aliquots of 9, 4, and 7 mg of acetophenone. The concentrations of acetophenone, **4**/**8**, and **10** were obtained from ^{1}H and ^{31}P-{^{1}H} NMR measurements.

RuH(*R*-binap)(η^5-$CH_2C(Ph)CHC(O)(Ph)$) (11). Acetophenone (100 mg, 0.83 mmol) was added to a solution of **5** (50 mg, 0.06 mmol) in benzene (1 mL). The mixture was left standing for 1 week at room temperature. Hexanes (10 mL) were then added, precipitating a yellow solid, which was filtered, washed with hexanes, and dried in vacuo (30 mg, 50%). ^{1}H NMR(C_6D_6) δ: −18.52 (dd, $^2J_{HP}$ = 24.3, 19.8 Hz, 1H, RuH), 2.63 (s, 1H CH_2), 3.80 (s, 1H CH_2), 5.62 (s, 1H CH), 6.28−8.35 (m, 32 H). ^{31}P{^{1}H} δ: 50.0 (d), 65.5 (d), $^2J_{PP}$ = 32.3 Hz. Crystals suitable for an X-ray diffraction study were obtained by layering a solution of **5** (20 mg) in acetophenone (100 mg) with hexanes.

RuH(PPh_3)$_2$(η^5-$CH_2CPhCHCPhO$) (12). This complex was observed in solution by reacting **4** with excess acetophenone in C_6D_6 for several days. ^{1}H NMR (C_6D_6) δ: −20.5 (dd, J_{H-P} = 32 Hz, 1H, RuH), 2.77 (d, J_{HH} = 3.6 Hz, 1H, CH), 3.38 (d, J_{HH} = 3.6 Hz, 1H, CH), 5.07 (s, 2H, CH), 6.7−7.9 (m, 40H, phenyl). ^{31}P{^{1}H} δ: 58.4 (d), 63.1 (d), J_{PP} = 22 Hz.

Reaction of 5 with 1-Phenylethanol. The addition of 1-phenylethanol (6 mg, 90% ee (*S*)) to a solution of the dihydride **5** (30 mg) in C_6D_6 (0.5 g) resulted, within 10 min, in the formation of the complex RuH(OCH(CH_3)Ph)(*R*-binap)(tmen) (**15a**) (30%) as a mixture of diastereomers (9:1) and broadening of the hydride chemical shift of **5** ($w_{1/2}$ 51 Hz) and the alcohol OH ($w_{1/2}$ 36 Hz). **15a** (major isomer). ^{1}H NMR δ: −17.0 (br, 1H, RuH). ^{31}P{^{1}H} δ: 67.8 (d), 73.8 (d), $^2J_{PP}$ = 42.6 Hz. **15a** (minor isomer). ^{1}H NMR δ: −17.15 (t, $^2J_{HP}$ = 25.8 Hz, 1H, RuH). ^{31}P{^{1}H} δ: 63.2 (d), 73.5 (d), $^2J_{PP}$ = 43 Hz.

Reaction of 4 with 1-Phenylethanol. Excess 1-phenylethanol was added to a solution of **4** (30 mg) in C_6D_6. Upon agitation the dark orange solution became a lighter yellow-orange color. The NMR spectra show an equilibrium mixture of the alkoxide species Ru(OCH(Me)-Ph)(PPh_3)$_2$(tmen) (**16a**), along with free 1-phenylethanol in fast exchange with **4** and an alcohol adduct **14a**. ^{1}H NMR of **16a** δ: −18.6 (t, J_{HP} = 25.95 Hz, 1H, RuH), 0.63 (s, 6H, CH_3), 0.88 (s, 6H, CH_3). ^{31}P {^{1}H} NMR δ: 69.9 (s).

Reaction of 5 with 2-Propanol. The addition of increasing aliquots of 2-propanol to a solution of **5** (30 mg) in C_6D_6 (0.5 g) resulted in the increasing formation of the isopropoxide complex RuH(^{i}PrO)(*R*-binap)-(tmen) (**15c**) with the evolution of hydrogen gas: 10 mg (7%), 100 mg (60%), 300 mg (90%). Addition of KOtBu to this mixture resulted in 50% regeneration of the dihydride complex **5**. **15c** ^{1}H NMR δ: −17.53 (t, $^2J_{HP}$ = 26.1 Hz, H, RuH). ^{31}P{^{1}H} δ: 62.7 (d), 73.1 (d), $^2J_{PP}$ = 42.8 Hz.

Reaction of 4 with *tert*-Butyl Alcohol. Approximately 1 equiv of *tert*-butyl alcohol was added to a solution of **4** in C_6D_6. This was stirred under Ar for 1 h during which time a gradual color change from dark orange-red to dark yellow took place. This resulted in an equilibrium mixture of **4** and the alkoxide species RuH(O^tBu)(PPh_3)$_2$(tmen) (**16b**), along with other decomposition products. ^{1}H NMR for **16b** δ: −17.7 (t, J_{HP} = 25.5 Hz, 1H, RuH). ^{31}P NMR δ: 70.4 (d).

Reaction of 4 with 2-Propanol. A suspension of **4** (50 mg) in 2-propanol (1 mL) was made under argon. The mixture was stirred under argon for 10 min. The color of the suspension changed from orange to yellow-green in less than 30 s. The solvent was removed in vacuo, leaving a green-yellow solid, which began to change back to orange under vacuum. ^{1}H and ^{31}P NMR of the residue were taken. A mixture of mostly **4**, and small amounts of **6**, RuH(O^iPr)(PPh_3)$_2$(tmen) (**16c**), and $RuH_4(PPh_3)_3$ were observed in the spectra. ^{31}P{^{1}H} NMR of **16c** (C_6D_6) δ: 70.7 (s).

***trans*-RuH(HCO_2)(*R*-binap)(tmen) (17).** A solution of formic acid (5 mg, 0.11) in THF (1 mL) was added to a solution of **5** (80 mg, 0.095 mmol) in THF (1 mL) and the mixture stirred for 30 min under nitrogen. Hexanes (5 mL) were added to the resulting solution, precipitating a bright yellow solid. This was filtered, washed with hexanes, and dried under vacuum. Yield = 62 mg, 74%. ^{1}H NMR δ: −19.05 (t, $^2J_{HP}$ = 25.9 Hz, H, RuH), 0.418 (s, 3 H, Me), 0.66 (s, 3 H, Me), 0.77 (s, 6 H, Me), 1.18 (d, $^2J_{HH}$ = 9.9 Hz, 1H, NH), 1.88 (d, $^2J_{HH}$ = 9.9 Hz, 1H, NH), 2.49 (d, $^2J_{HH}$ = 9.9 Hz, 1H, NH), 7.57 (d, $^2J_{HH}$ = 9.9 Hz, 1H, NH), 6.18−8.51 (m, 32 H), 9.52 (s, 1H, HCO_2). ^{31}P{^{1}H} δ: 65.2 (d), 69.9 (d), $^2J_{PP}$ = 45.3 Hz. IR (Nujol, cm^{-1}) 3342, 3310, 3283 (N−H), 1589 (C═O). Anal. Calcd: C, 69.1; H, 5.7; N, 3.2. Found: C, 68.9; H, 5.7; N, 2.9.

***trans*-RuH(HCO_2)(PPh_3)$_2$(tmen) (18).** Formic acid (2 mg) and **4** (32 mg) were added to an NMR tube and dissolved in deuterated benzene under Ar. The dark orange-red solution evolved gas (hydrogen and carbon dioxide) and quickly turned yellow. The ^{1}H and ^{31}P NMR spectra were obtained. The solution was layered with hexanes under argon. Slow diffusion into hexanes yielded yellow crystals from which an X-ray crystal structure was obtained. ^{1}H NMR (C_6D_6) δ: −19.8 (t, J_{H-P} = 25 Hz, 1H Ru−H), 0.6 (s, 6H, CH_3), 0.8 (s, 6H, CH_3), 2.0 (d J_{H-H} = 10 Hz, 2H, NH), 5.0 (d, J_{H-H} = 10 Hz, 2H, NH), 6.8−8.0 (m, 30H, phenyl), 9.3 (s, 1H, formate CH). ^{31}P{^{1}H} NMR (C_6D_6) δ: 69.3 (s, PPh_3). IR (Nujol, cm^{-1}) 3337, 3320, 3276 (N−H), 2011 (Ru−H), 1589 (C═O).

Kinetics. Hydrogenation reactions were carried out at constant pressures of H_2 using a 50 mL Parr hydrogenation reactor or a Schlenk flask. Standard solutions of acetophenone (0.833 M) and **5** (2.28×10^{-3} M) or **4** (1.35×10^{-2} M) were prepared by dissolving the required amount of compound in 10 mL of C_6D_6. Reaction mixtures were prepared by pipetting the required amounts of ketone, dihydride (or amido) complex, and C_6D_6 to give a final volume of 5 mL upon mixing. The Parr hydrogenation reactor was flushed several times with hydrogen gas at the pre-set pressure prior to adding the reaction mixture or its components. There was no significant change in rate if the components of reaction mixture were mixed together or added separately. Aliquots of the reaction mixture were quickly withdrawn with a syringe under a flow of hydrogen at regular time intervals (the minimum interval was 60 s) by venting the Parr reactor. Sampling times ranged from 5 to 10 s during which time the pressure dropped to near atmospheric pressure. Concentrations of 1-phenylethanol and acetophenone were determined by ^{1}H NMR or gas chromatography. Constant temperatures were maintained using a constant temperature water bath.

Computation. All computations were carried out with the pseudospectral Jaguar 4.0 and 4.1 program packages[64] using density functional theory (DFT). For the small model system (L = PH_3, diamine = en), geometry optimization was carried out using the standard B3LYP hybrid density functional with the Jaguar LACVP* basis sets[64] (Los Alamos ECP + split-valence basis set for the outermost 4s, 4p, 4d, and 5s electrons, split-valence polarized 6-31G* basis set on all other atoms, = BS A). A subsequent frequency run at the same level was used to derive zero-point energy corrections and to check the nature of minima and transition states. More accurate energetics were derived from single-

(64) Schrödinger, Inc., Portland, OR, 1996−2001.

point energies using the LACV3P++ basis on Ru (this is a triple-ζ version of the LACVP ECP basis set developed for use with Jaguar, with one additional set of diffuse d functions[64] and the standard 6-311+G** triple-ζ basis on all other atoms (= BS B). For greater accuracy, the "fine" DFT and "ultrafine" pseudospectral grids were used for all energy calculations. Some stationary points were studied also using the "pure" BP86 density functional and BS A, to check that the results are not excessively functional-dependent.[65]

For the large systems (L = PPh_3 or BINAP, diamine = en, tmen), all calculations were carried out using the B3LYP functional, and with a carefully chosen basis set (BS C) to minimize computational expense but provide the most accurate description of the metal and its environment. Thus, the triple-ζ LACV3P Jaguar ECP and basis set were used on Ru,[64] with the 6-31G basis on all other atoms. Polarization functions were added on selected atoms: the hydride and NH_2 groups, the phosphorus atoms, the CO_2 molecule, and the formate group were treated with the 6-31G** basis. For comparison of the overall reaction energy with that of the model system, the 6-31G** basis was used on the acetophenone and 1-phenylethanol reactant and product, respectively. For the large system, geometry optimization was carried out using the "loose" geometry convergence criteria in Jaguar (e.g., rms gradients below 1.5×10^{-3} Hartree/Bohr[64]); test calculations using default convergence criteria led to negligible differences in energies, bond lengths, and bonding angles. Final energies at the optimized geometries were computed using the same basis set BS C, together with the tightest DFT and pseudospectral grids. Frequency calculations on these large systems are prohibitively expensive and have not been carried out. Further details, including optimized structures and total energies, are included in the Supporting Information.

(65) Koch, W.; Holthausen, M. C. *A Chemist's Guide to Density Functional Theory*; Wiley-VCH: Weinheim, 2000.

Acknowledgment. This work was supported by grants to R.H.M. from NSERC Canada and PRF, as administered by the American Chemical Society, and by a donation of *R*-binap from Digital Chemical Co. and a loan of $RuCl_3$ from Johnson-Matthey. We thank Michael Faatz for some preliminary work and Dr. Timothy Burrow for carrying out some NMR experiments.

Supporting Information Available: Tables of equilibrium and kinetic data. X-ray structural information for complexes **2**, **4**, **8**, and **9**. Cartesian coordinates and total electronic energies for the computed species. An X-ray crystallographic file (CIF). This material is available free of charge via the Internet at http://pubs.acs.org.

JA016817P